No. 030

September 1969

OSCILLATING PRESSURE FIELDS ON A FREE SURFACE

T. Francis Ogilvie

This research was carried out
in part under the
Naval Ship Systems Command
General Hydromechanics Research Program
Subproject SR 009 01 01, administered by the
Naval Ship Research and Development Center.
Contract No. N00014-67-A-0181-0016
Reproduction in whole or in part is permitted
for any purpose of the United States Government.

This document has been approved for public release
and sale; its distribution is unlimited.

Department of Naval Architecture
and Marine Engineering
College of Engineering
The University of Michigan
Ann Arbor, Michigan 48104

ABSTRACT

The effect of a vertical barrier or lip on the wave generating capability of a pneumatic wavemaker is analyzed. For lip immersion approaching zero, the wave amplitudes approach the values predicted by Stoker in 1957. For finite lip immersion, wave amplitude is generally reduced below the amplitude from a wavemaker with no lip, but under certain conditions the amplitude can be greatly increased by the lip. Numerical results are presented.

These results are used to show that the effect of sidewalls will be generally negligible in predicting the added mass and damping per unit length of a long air-cushion vehicle with sidewalls (captured-air-bubble vehicle). Such effects then being neglected, the added mass and damping are computed as functions of frequency and conditions of static support. The amplitude and phase of the mean free surface motion under the vehicle are also computed. It is found that the surface motion can actually be exactly opposite to that expected from quasi-static considerations.

PREFACE

At a meeting of the H-5 Panel of the Society of Naval Architects and Marine Engineers in June, 1969, I heard Dr. John Breslin* discuss a current problem of air-cushion-vehicle (ACV) research, *viz.*, the prediction of the added-mass and damping coefficients of an inverted box heaving on an air-water interface. The air trapped under the box suffers a variable pressure, causing waves to be generated on the free surface. The hydrodynamic response causes a reaction on the box (again through the captured air). It is this reaction which one needs to know in order to calculate the motions characteristics of the vehicle.

One aspect of this problem is very similar to a problem which I solved several years ago. In 1962, I was concerned with the effect of a vertical barrier or lip on the wave generating capability of a pneumatic wavemaker. It was immediately clear that the sides of the box containing the captured air bubble would have effects qualitatively similar to the effects of the wavemaker lip. The earlier calculations indicated, in fact, that such effects would be rather unimportant in the range of parameters relevant to the ACV problem. This conclusion alone seemed to be of sufficient significance to warrant publishing the calculations. Furthermore, the conclusion justifies using a very simple mathematical model for the air bubble and its interaction with water and vehicle.

It then proved possible to formulate and solve completely the two-dimensional problem of predicting the added-mass and damping coefficients of the vehicle. It would be only a modest extension of these results to use them as the basis for a strip theory for predicting the motions of an idealized ACV. This last step is not carried out here; only the 2-D

---

*Director, Davidson Laboratory, Stevens Institute of Technology, Hoboken, N. J.

(strip) results had been obtained when the effort was terminated at the beginning of July.

I am greatly indebted to two people for the computations on which this report is based:

Mrs. P. M. Monacella performed the wavemaker computations in 1962 at the David Taylor Model Basin. This was a very complicated task, involving, for example, many incomplete elliptic integrals. It is an indication of the thoroughness of her work that it was possible after nearly seven years to retrieve her papers from the files and immediately use them!

Mr. Young Tsun Shen performed the added-mass and damping coefficient calculations on the computer at the University of Michigan. He delivered the results to me (hand-checked) less than twenty-four hours after I stated the problem to him.

One is very fortunate to be able to work with people such as Mrs. Monacella and Mr. Shen.

T. Francis Ogilvie

CONTENTS

INTRODUCTION

This report presents the solutions of several problems involving oscillatory pressure distributions applied on the free surface of infinitely deep water. A considerable part of this work was done in 1962 as part of a project to optimize the pneumatic wavemakers at the David Taylor Model Basin. (See Figure 1). Accordingly, attention was centered then on the problem of predicting the waves generated by a sinusoidally varying pressure field applied uniformly over a section of the free surface. The results were never published, because the problem did not appear to have widespread interest. However, the calculations now possibly have new value in a problem involving the motions of an air-cushion vehicle. Therefore we are presenting these calculations here, along with their extension and application to the air-cushion-vehicle problem.

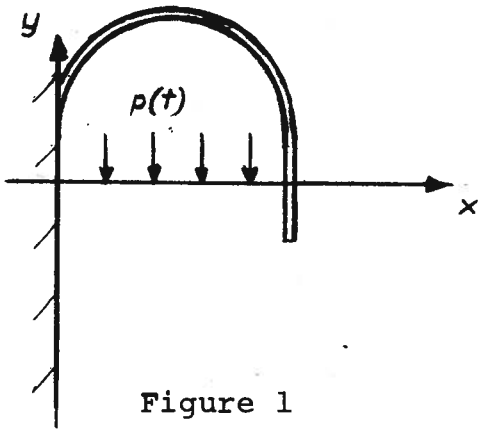

Figure 1

In the wavemaker problem, the simplest mathematical model has been discussed fully by Stoker (1957): A sinusoidally varying pressure is applied to a segment of the free surface, and the resulting water motion (including radiated waves) is computed; the usual assumptions of linearized water-wave theory are made.

Perhaps the most important deficiency of this mathematical model is the neglect of the barrier which is necessary physically in order for a pressure field to be applied on a restricted region of the free surface. In our original study in 1962, the main goal was to predict the effect of the wavemaker lip on the efficacy of the wavemakers. The lip is nothing more than a vertical barrier plate which penetrates the free surface. The generalization from Stoker's problem consisted solely of introducing the mathematical equivalent of such a barrier.

The results of these calculations are presented in Figures 7 and 8. It is found that:

a) The amplitude of the generated waves goes to zero as νa approaches an integer multiple of π, where ν is the wave number of the generated waves and a is the width of the wavemaker (the region to which the pressure is applied). This result was found in the simpler problem described by Stoker. (See Equation (9) in the next section.)

b) The barrier generally reduces the amplitude of the generated waves, especially if the corresponding wavelengths are smaller than or comparable with the immersion of the barriers. This result was to be expected.

c) If the generated waves are much longer than the wavemaker width, the amplitude of the generated waves can be considerably augmented by the presence of the lip. What is perhaps more surprising is that the maximum amount of augmentation increases as lip immersion increases. However, the range of wavelengths in which this phenomenon occurs becomes smaller and smaller as lip immersion increases, and the range moves in the direction of longer and longer waves.

d) For small lip immersion, there can even be an augmentation in the amplitude of short-wavelength waves. This effect is very pronounced if the value of νa is just slightly greater than π. Again, the augmentation is greater, although over a smaller range of wave-lengths, for

increasing values of lip immersion.

The results described in c) and d) above suggest that there is some kind of resonance phenomenon occurring. Calculations have not been made for the free-surface motion under the wavemaker, but one may suppose that the surface oscillation is rather violent, much more so than one might expect on the basis of Stoker's analysis. Otherwise, the barrier would serve only to reduce the amount of energy which could escape from the wavemaker in the form of radiated waves. Qualitative observations with a pneumatic wavemaker at the University of Michigan indicate that the resonance hypothesis is plausible.

This unexpected behavior will possibly not be predicted accurately by the theory, since the latter is based on the hypothesis of an ideal fluid. Because of this hypothesis, the theory predicts infinite velocity around the barrier edge. One may expect this unreasonable prediction to lead to errors which are primarily local in scope if the amplitude of motion is quite small. A more rational, but still qualitative, condition is that free vortices should not wander far from the sharp barrier edges if the analysis is to have any relevance to the physical problem. Violent motion around the barrier certainly precludes a quantitative application of the theory; how far the qualitative predictions are invalidated can hardly be predicted.

A simple extension of the wavemaker analysis allows one to solve another class of problems: Computation of the reflection and transmission of waves incident broadside on a pair of vertical surface-piercing barriers. The analysis is carried out here, although no numerical results are presented. This problem has been solved in a different way by Levine and Rodemich (1958).

If we add to the wavemaker considered here its image with respect to the vertical axis, the problem becomes nearly

equivalent to the problem of a heaving, very long air-cushion vehicle. As an idealization, we consider a box of infinite length, with base and two sides, inverted over the water, oscillating vertically. The air trapped under the box will undergo oscillatory compressions which have the same effect on the water as the varying pressure in the wavemaker. We cannot immediately relate the pressure fluctuations to the box motions, since the pressure will depend also on the response of the water surface. Nevertheless, it will be shown how the problem can be completely solved, ending finally with simple formulas for the added-mass and damping coefficients for the box. A set of curves is presented, showing how these coefficients depend on νa and on the static conditions of support of the box. (Note that a is here the half-beam of the box.) See Figures 10 and 11.

Our analysis for the inverted-box problem is based on Stoker's simple mathematical model for the wavemaker. This was largely a matter of expedience, because the corresponding calculations for the wavemaker-with-lip problem would have been quite lengthy. However, it should be observed that the latter would not be strictly appropriate either, because the sides of the box oscillate along with the base of the box, whereas the edges of the barriers are fixed in the wavemaker problem.

Nevertheless, the detailed calculations presented for the wavemaker-with-lip problem serve an important function in suggesting the nature and extent of sidewall effects. For $\nu a < 1$ (which implies wavelength $> 2\pi a$) and $b/2a < 0.1$, the wave-producing capability of the wavemaker is essentially unaffected by the lip. It is probably reasonable to assume that, under the same condition, the box sidewalls do not greatly affect the force on the box base. The conditions of interest in the air-cushion-vehicle problem are not likely to be excluded by these

restrictions, and so the analysis should provide a valid guide to the magnitude of the oscillatory force on the box base.

A word of caution is necessary about the application of these results. They have a strong similarity in nature to the stripwise added-mass and damping per-unit-length coefficients that are commonly used in ship-motion theory. It is well known that strip theory provides a reliable basis for approaching the prediction of ship motions, and so it is tempting to use these results in the same way for predicting the motions of an air-cushion vehicle. However, a number of reasons can be cited for believing that this will not be a straightforward matter; for example:

1) There is a strong coupling between stations, because the pressure of the cushion is approximately constant within any single chamber under the vehicle. By contrast, each cross-section of a ship is initially fixed geometrically, and interactions between stations come about only through hydrodynamic effects and through the rigid-body dynamics of the ship.

2) The pressure is here assumed to vary only with the enclosed volume, in accordance with the adiabatic gas law. The use of this law is perhaps not unjustified, but there are certainly other very important factors which affect the pressure, such as the response of the fans to variable back pressure and the leakage of air at the bow and stern (and possibly under the sidewalls).

For such reasons, the analysis herein is not presented as a method for computing the stripwise added-mass and damping coefficients for an air-cushion vehicle. That will be a more complicated problem — if indeed the strip approach can be used at all with any reasonable validity.

THE FOUR BASIC PROBLEMS

In this section we present the solutions of four basic problems:

(1) An oscillating pressure field applied to a segment of the free surface.

(2) An oscillating pressure field applied to a segment of the free surface, the segment being bounded by vertical barriers of specified depth.

(3) Horizontally symmetric standing waves which can exist in the presence of the barriers of problem (2).

(4) Horizontally antisymmetric standing waves which can exist in the presence of the barriers of problem (2).

Problem (1) was solved many years ago by Stoker (1957), and we only quote his results here. The solution satisfies the condition that there be only outgoing waves at infinity.

For problem (2), we obtain a particular solution, without regard to the existence of any prescribed conditions at infinity. The solution will represent standing waves, not outgoing waves, at great distances from the region of the applied pressure. However , the solution can be combined with the solution of problem (3) to yield an appropriate outgoing-wave solution.

The solutions of problem (3) and (4) can be combined to provide the solution of the problem of incident waves on a pair of barriers. See Levine and Rodemich (1958) for a different method of solution.

(1) Oscillating pressure on the free surface

Let there be a pressure distribution on the free surface

$$p(x,t) = \begin{cases} P \sin \omega t \ , & |x| < a \ , \\ 0 \ , & |x| > a \ . \end{cases} \qquad (1)$$

See Figure 2. We seek a velocity potential, $\phi(x,y,t)$, satisfying a) the Laplace equation in $y < 0$ and b) the following free-surface boundary condition:

$$\phi_y - \nu\phi = -(1/\rho g)p_t(x,t) = \begin{cases} -\frac{\omega P}{\rho g}\cos\omega t\ , & |x| < a\ ; \\ 0\ , & |x| > a\ , \end{cases} \tag{2}$$

where $\nu = \omega^2/g$. It is convenient to write the potential in the following way:

$$\phi(x,y,t) = \phi_1(x,y)\sin\omega t + \phi_2(x,y)\cos\omega t\ .$$

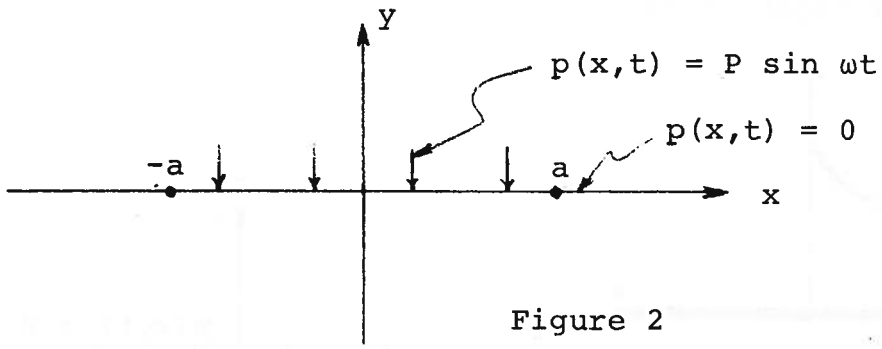

Figure 2

Then the boundary conditions on ϕ_1 and ϕ_2 are:

$$\phi_{1_y} - \nu\phi_1 = 0\ , \qquad -\infty < x < \infty\ ,\ y = 0\ ; \tag{3}$$

$$\phi_{2_y} - \nu\phi_2 = \begin{cases} -\omega P/\rho g\ , & |x| < a\ ,\ y = 0\ ; \\ 0\ , & |x| > a\ ,\ y = 0. \end{cases} \tag{4}$$

We require that the solution represent outgoing waves as $|x| \to \infty$ and that the fluid velocity vanish as $y \to -\infty$

The solution, as given by Stoker (1957), is:

$$\phi_1(x,y) = -(2P/\rho\omega)\ \sin \nu a\ e^{\nu y}\ \cos \nu x\ ; \qquad (5)$$

$$\phi_2(x,y) = Re\{f(z)\} - (2P/\rho\omega)\ \sin \nu a\ e^{\nu y}\ \sin \nu x\ ; \qquad (6)$$

the complex potential, $f(z)$, is given by:

$$f(z) = -(\omega P/\pi\rho g)\ e^{-i\nu z} \int_{C_{i\infty}}^{z} dt\ e^{i\nu t}\ \log \frac{t-a}{t+a}\ , \qquad (7)$$

where, for $y < 0$, the contour is always taken around the left side of the cut between $z = -a$ and $z = +a$; see Figure 3. We take the principal branch of the logarithms: $-\pi \leq \arg(t \pm a) \leq +\pi$.

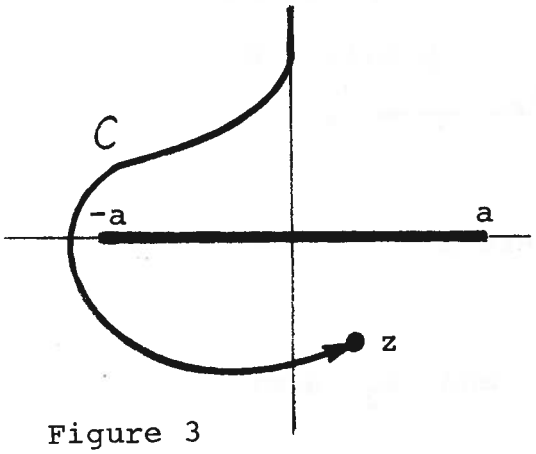

Figure 3

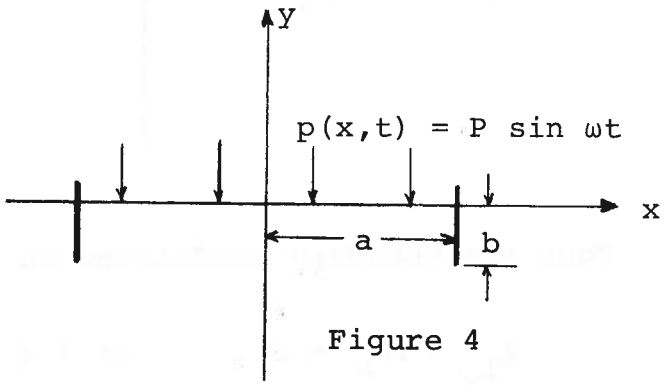

Figure 4

The free surface deflection is given by:

$$\eta(x,t) = (\omega/g)\ [\phi_2(x,0)\ \sin \omega t - \phi_1(x,0)\ \cos \omega t\ ] - (1/\rho g)\ p(x,t)\ . \qquad (8)$$

As $x \to \pm \infty$, this reduces to:

$$\eta(x,t) = (2P/\rho g)\ \sin \nu a\ \cos(\omega t \mp \nu x) + O(1/x)\ . \qquad (9)$$

For $|x| < a$, we find that:

$$\eta(x,t) = [-P/\rho g + (\omega/g)\ Re\{f(x-i0)\} - (2P/\rho g) \sin \nu a \sin \nu x] \sin \omega t + [(2P/\rho g) \sin \nu a \cos \nu x] \cos \omega t \ . \tag{10}$$

If this problem is taken as a mathematical model for a pneumatic wavemaker, Equation (9) provides a means of predicting the amplitude of waves which will be generated. The model is admittedly rather crude. Besides the usual restrictions of linearized water-wave theory, the model leads to singularities at the edges of the wavemaker. However, these singularities are very weak, and so one may hope that the resulting errors are quite local in scope.

(2) Oscillating pressure field between barriers

This problem introduces a presumably better mathematical model for the same physical situation considered in the above problem. If a uniform pressure field is to be applied on a segment of the free surface, it will be necessary in practice to enclose that segment within walls penetrating the free surface. Therefore we study the problem depicted in Figure 4. There are two barriers of zero thickness located at $x = \pm a$, extending from above the free surface to a depth b below the undisturbed free surface. The oscillating pressure field is applied between the two barriers. We may consider that the y -axis is replaced by a solid wall, and so we seek a solution which is symmetrical about the y -axis.

It should again be noted that the solution to this problem is still not an entirely satisfactory solution of the physical problem. There will be singularities at the lower edges of the barriers, implying fluid velocities which vary

in magnitude inversely with the square root of the distance from those edges. Thus the solution will have meaning only if the effects of the edges are really local.

We shall seek a particular solution of the problem, not concerning ourselves with the radiation condition — for the moment. In problem (3), below, we shall find a solution of the homogeneous problem ($p(x,t) = 0$) which can be combined with the solution of the present problem to represent the outgoing-wave solution appropriate to the wavemaker problem.

We shall show that a particular solution can be found if we take the form of the velocity potential to be: $\phi(x,y) \cos \omega t$. The free-surface boundary condition will be the same as Equation (4):

$$\phi_y - \nu\phi = \begin{cases} -(\omega P/\rho g) , & |x| < a , \quad y = 0 ; \\ 0 , & |x| > a , \quad y = 0 . \end{cases} \tag{11}$$

There will now be a boundary condition on the barriers:

$$\phi_x = 0 , \qquad x = \pm a , \quad -b < y < 0 ,$$

and a similar condition on the negative y -axis, either because we require a symmetric solution or because we consider the y -axis to be a rigid wall:

$$\phi_x = 0 , \qquad x = 0 , \quad y < 0 .$$

These two conditions are equivalent to setting the stream function equal to a constant on each of these boundaries. We are always free to add a constant to the stream function, and so we may as well set

$$\psi = 0 , \qquad x = 0 , \quad y < 0 , \tag{12}$$

where $\psi(x,y)$ is the stream function which is the complex conjugate function to $\phi(x,y)$. The value of the stream function on the barriers is not necessarily zero, but, if we can find a solution which does satisfy the condition:

$$\psi = 0 , \qquad x = \pm a , \quad -b < y < 0 , \tag{13}$$

that solution will serve perfectly well as our *particular* solution. In fact, we *can* find such a solution, and so we impose (13) as a boundary condition of our problem.

We expect singularities at the lower edges of the barrier, and, as usual in such problems, we demand that the singularities be as weak as possible. It turns out that we must allow square-root infinities in the velocity, and so we have the condition that:

$$\left[(x\mp a)^2 + (y+b)^2\right]^{1/2} |\nabla\phi| \text{ be bounded near } \begin{cases} x = \pm a , \\ y = -b . \end{cases} \tag{14}$$

We require that the velocity be bounded everywhere else in the lower half-space and that the velocity vanish as $y \to -\infty$.

To solve this problem, we use the "reduction method" (See Stoker (1957) or Wehausen and Laitone (1960)), carrying out the actual solution in an image plane which is obtained from the physical plane by a simple conformal mapping.

To begin, we state the problem in terms of functions of a complex variable. Let

$$(\omega P/\rho g)\ f_2(z) = \phi(x,y) + i\psi(x,y) , \tag{15}$$

The boundary conditions can be stated in terms of $f_2(z)$ as follows:

$$Im\{f_2'(z) + i\nu f_2(z)\} = \begin{cases} 1 , & |x| < a , \ y = 0 ; \\ 0 , & |x| > a , \ y = 0 ; \end{cases} \tag{11'}$$

$$Im\{f_2(z)\} = 0 \ , \quad x = 0 \ , \quad y < 0 \ ; \tag{12'}$$

$$Im\{f_2(z)\} = 0 \ , \quad x = \pm a \ , \quad -b < y < 0 \ ; \tag{13'}$$

$$|z - (\pm a - ib)| \ |f_2'(z)| \ \text{ bounded near } \ z = \pm a - ib \ . \tag{14'}$$

In place of (12') and (13'), we note that we can write:

$$Re\{f_2'(z) + i\nu f_2(z)\} = 0 \ , \quad x = 0 \ , \quad y < 0 \ ; \tag{12"}$$

$$Re\{f_2'(z) + i\nu f_2(z)\} = 0 \ , \quad x = \pm a \ , \ -b < y < 0 \ . \tag{13"}$$

We can now define a new function on which the boundary conditions are quite simple:

$$g_2(z) \equiv f_2'(z) + i\nu f_2(z) \ . \tag{16}$$

Since $g_2(z)$ is just the same as the expression in braces in (11'), (12"), and (13"), the boundary conditions on $g_2(z)$ involve simply the values of its real and imaginary parts. The essence of the "reduction method" is the determination of this simpler function, $g_2(z)$; when this has been accomplished, we reinterpret the definition of $g_2(z)$, Equation (16), as a differential equation to be solved for $f_2(z)$.

From (11') and (16), we have the condition that $Im\{g_2(z)\} = 0$ on the real axis outside of the wavemaker segment. By the Schwartz reflection principle, we can then continue $g_2(z)$ analytically into the upper half-plane according to the prescription:

$$g_2(\bar{z}) = \overline{g_2(z)}$$

This in turn implies that $Im\{g_2(z)\} = \mp 1$ on the cut, that

is, on $y = \pm 0$, $|x| < a$. Thus, $Im\{g_2(z)\}$ has a jump in its value across the cut in the complex plane. The conditions on the vertical axis and on the barrier can be continued unchanged into the upper half-plane, since $Re\{g_2(z)\}$ is an even function of y .

The generalized conditions on $g_2(z)$ are now the following:

$$Im\{g_2(z)\} = \mp 1 , \quad y = \pm 0 , \quad |x| < a ; \tag{18}$$

$$Im\{g_2(z)\} = 0 , \quad y = 0 , \quad |x| > a ; \tag{19}$$

$$Re\{g_2(z)\} = 0 , \quad x = 0 , \quad -\infty < y < \infty ; \tag{20}$$

$$Re\{g_2(z)\} = 0 , \quad x = \pm a , \quad -b < y < +b . \tag{21}$$

In addition, from (14') and the analytic continuation, it is apparent that $g_2(z)$ may be expected to have square-root infinities at the four edges of the extended barriers, that is, at $(\pm a,-b)$ and $(\pm a,+b)$.

The $g_2(z)$ -problem can be reduced to an even simpler one by a Schwartz-Christoffel transformation:

$$\frac{dz}{d\zeta} = \frac{\zeta^2-\gamma^2}{\sqrt{(\zeta^2-\alpha^2)(\zeta^2-\beta^2)}} . \tag{22}$$

To make the mapping unique, we integrate (22) as follows:

$$z(\zeta) = \int_0^{\zeta} \frac{(t^2-\gamma^2)\,dt}{\sqrt{(t^2-\alpha^2)(t^2-\beta^2)}} . \tag{23}$$

It does not matter what contour we follow in this integration, provided we do not cross the two cuts in the ζ -plane which are the images of the barriers in the z -plane. Figure 5

shows some corresponding points in the two planes. Various properties of the mapping are discussed in Appendix A.

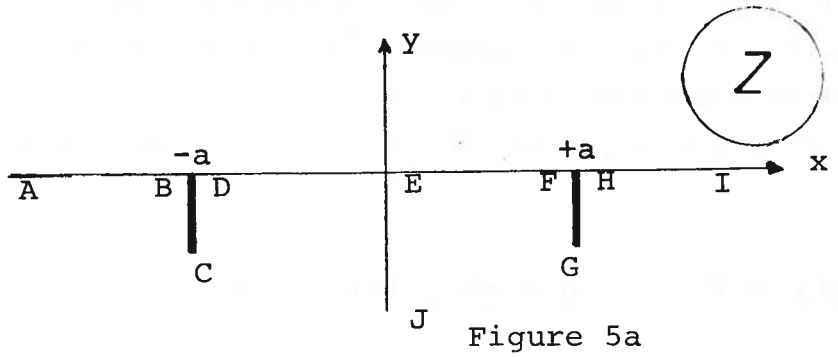

Figure 5a

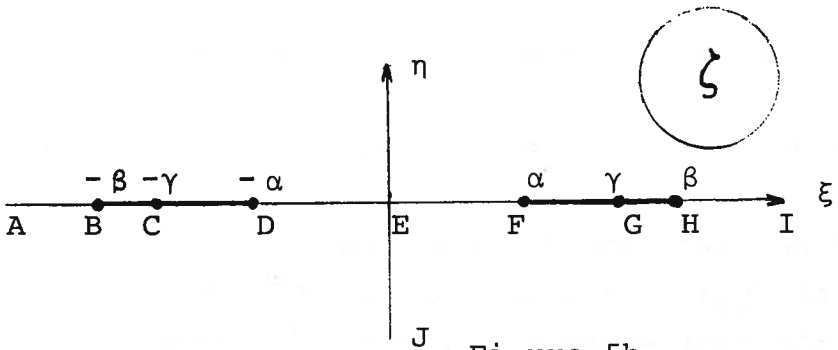

Figure 5b

We define two functions of ζ :

$$G_2(\zeta) = g_2(z(\zeta)) \ ; \tag{24}$$

$$F_2(\zeta) = f_2(z(\zeta)) \ . \tag{25}$$

The simple boundary conditions on $g_2(z)$ are, of course, retained by $G_2(\zeta)$ in the mapping, and so, corresponding to (18)-(21), we have:

$$Im\{G_2(\zeta)\} = \mp 1 \ , \quad \eta = \pm 0 \ , \ |\xi| < \alpha \ ; \tag{18'}$$

$$Im\{G_2(\zeta)\} = 0 \ , \quad \eta = 0 \ , \ |\xi| > \beta \ ; \tag{19'}$$

$$Re\{G_2(\zeta)\} = 0 \ , \quad \xi = 0 \ , \ -\infty < \eta < \infty \ ; \tag{20'}$$

$$Re\{G_2(\zeta)\} = 0 \ , \quad \eta = 0 \ , \ \alpha < |\xi| < \beta \ . \tag{21'}$$

It is not so obvious -- but nevertheless true -- that:

$$|\zeta \pm \gamma||G_2(\zeta)| \ \text{ is bounded near } \ \zeta = \pm\gamma \pm i0 \ . \tag{26}$$

The points mentioned in (26) are the images of the barrier ends and of their reflections about the real axis.

With the boundary conditions now expressed in terms of values of the function $G_2(\zeta)$ on the axes only, the problem is easily solved by the methods discussed by Muskhelishvili (1953). The solution is:

$$G_2(\zeta) = -\frac{1}{\pi}\frac{\sqrt{(\zeta^2-\alpha^2)(\zeta^2-\beta^2)}}{\zeta^2-\gamma^2}\int_{-\alpha}^{\alpha}\frac{(t^2-\alpha^2)dt}{(t-\zeta)\,|(\alpha^2-t^2)(\beta^2-t^2)|^{1/2}} \tag{27}$$

$$= -\frac{2\zeta}{\pi}\frac{\sqrt{(\zeta^2-\alpha^2)(\zeta^2-\beta^2)}}{\zeta^2-\gamma^2}\int_{0}^{\alpha}\frac{(t^2-\gamma^2)dt}{(t^2-\zeta^2)\,|(\alpha^2-2)(\beta^2-t^2)|^{1/2}} \tag{27'}$$

This solution is not mathematically unique, but, following Muskhelishvili, we can show that the other possibilities violate conditions necessary at infinity. The correctness of these expressions can be verified by use of the Plemelj formulas (again, see Muskhelishvili), without the necessity of deriving solutions.

From the definition of $g_2(z)$, Equation (16), we obtain a differential equation for $F_2(\zeta)$:

$$f_2'(z) + i\nu f_2(z) = \frac{d\zeta}{dz}F_2'(\zeta) + i\nu F_2(\zeta) = g_2(z) = G_2(\zeta) \ .$$

Slightly rewritten, this is:

$$F_2'(\zeta) + i\nu\frac{dz}{d\zeta} F_2(\zeta) = \frac{dz}{d\zeta} G_2(\zeta) \ . \qquad (28)$$

The general solution is:

$$f_2(z) = F_2(\zeta) = e^{-i\nu z(\zeta)} \left(\int_{0-i0}^{\zeta} e^{i\nu z(t)} \ \frac{dz}{dt} G_2(t) \ dt + K_2 \right) ,$$

where K_2 is a complex constant yet to be determined. The lower limit of the integral in the solution has been arbitrarily set for later convenience. The contour of the integration must not cross the real axis between $\pm \beta$, because this is a branch cut of the integrand.

From Equation (12'), we find that:

$$Im\{K_2\} = 0 \ ,$$

and from Equation (13') it follows that:

$$K_2 = (1/\nu) - (\sin \nu a)^{-1} \int_{0-i0}^{\alpha-i0} dt \ \frac{dz}{dt} \sin \nu[a-x(t)][G_2(t)-i] \ . \qquad (29)$$

Thus, the solution for $f_2(z)$ is:

$$f_2(z) = e^{-i\nu z} \left(\int_{0-i0}^{\zeta} dt \ \frac{dz}{dt} e^{i\nu z(t)} G_2(t) + (1/\nu) \right.$$
$$\left. + (\sin \nu a)^{-1} \int_{0-i0}^{\alpha-i0} dt \ \frac{dz}{dt} \sin \nu[a-x(t)][G_2(t)-i] \right) . \qquad (30)$$

This is the complete solution of problem (2).

We shall need to know the behavior of the solution as $x \to \pm\infty$. From Appendix A we have that:

$$z = \zeta + O(1/z) \qquad \text{as} \quad |z| \to \infty \ .$$

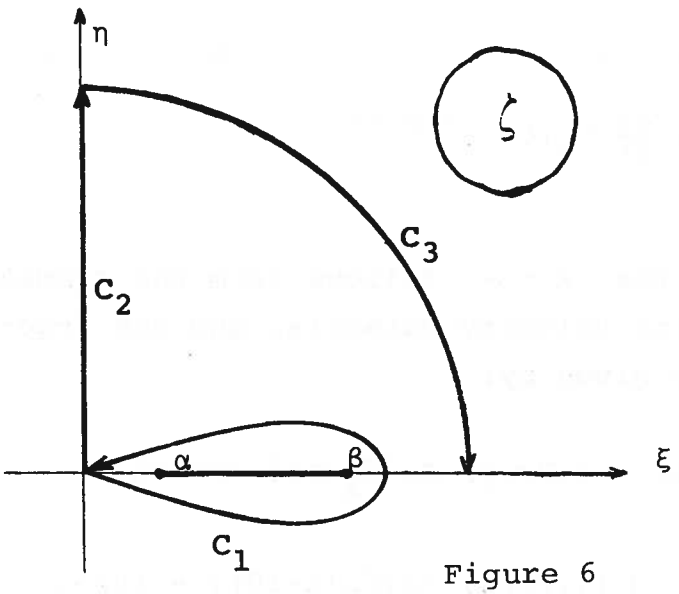

Figure 6

We deform the contour of integration in (30) as shown in Figure 6. The integral along C_3 vanishes as the radius of C_3 increases to infinity, leaving only the integrals along C_1 and C_2. The first of these contours can be shrunk down to the real axis, and the properties of $G_2(\zeta)$ and $z(\zeta)$ can be used to simplify the integrals. The result is the following:

$$Re\{f_2(z)\} \sim e^{\nu y} [A_2 \cos \nu x \pm B_2 \sin \nu x], \quad \text{as } x \to \pm \infty , \tag{31}$$

where

$$A_2 = (2/\nu)(\cos \nu a - 1) + D_2 \cos \nu a + E_2 + K_2 , \tag{31a}$$

$$B_2 = (2/\nu) \sin \nu a + D_2 \sin \nu a , \tag{31b}$$

$$D_2 = -\int_{\alpha-i0}^{\beta-i0} dt \, \frac{dz}{dt} \, G_2(t) [e^{\nu y(t)} - e^{-\nu y(t)}] , \tag{31d}$$

$$E_2 = \int_0^{i\infty} dt \, \frac{dz}{dt} \, G_2(t) \, e^{-\nu y(t)} \quad . \tag{31e}$$

(The result for $x \to -\infty$ follows from the symmetry of the problem.) The velocity potential and the free-surface disturbance are given by:

$$\phi(x,y,t) = (\omega P/\rho g) \, Re\{f_2(z)\} \cos \omega t \; ; \tag{32}$$

$$\eta(x,t) = \begin{cases} [(\nu P/\rho g) \, Re\{f_2(x-i0)\} - (P/\rho g)] \sin \omega t \; , & |x| < a \; , \\ (\nu P/\rho g) \, Re\{f_2(x-i0)\} \sin \omega t \; , & |x| > a \; . \end{cases} \tag{33}$$

(3) Symmetrical standing waves in presence of barriers

The geometry of the boundaries is the same as in the previous problem; see Figure 4. However, we now assume that the pressure distribution is identically zero over the whole free surface, and so the free-surface boundary condition is:

$$\phi_y - \nu\phi = 0 \; , \qquad y = 0 \; , \quad -\infty < x < \infty \; .$$

Again we seek a solution which would be appropriate if there were a rigid wall on the y-axis, and so we again require that:

$$\phi_x = 0 \; , \quad x = 0 \; , \quad y < 0 \; ,$$

or, what is equivalent,

$$\psi = 0 \; , \quad x = 0 \; , \quad y < 0 \; , \tag{34}$$

where ψ is the stream function conjugate to ϕ .

On the barriers, we again have that $\phi_x = 0$, or the equivalent, that ψ is a constant. It will not do now to set $\psi = 0$ on the barriers, for it can be shown that the only possible result would be the trivial one that ϕ equals a constant (everywhere). Therefore we must take a non-zero value for ψ on the barriers. Since the problem is linear and homogeneous, it does not matter what value we take, and so we choose the convenient value:

$$\psi = -1/\nu \ , \quad x = a \ , \quad -b < y < 0 \ . \tag{35}$$

From equation (34), it is apparent that ψ must be odd with respect to x , and so we can extend (35):

$$\psi = \mp 1/\nu \ , \quad x = \pm a \ , \quad -b < y < 0 \ . \tag{35'}$$

The solution procedure is just the same as in problem (2): We define the complex potential:

$$f_3(z) = \phi(x,y) + i\psi(x,y) \ ,$$

and the reduced function,

$$g_3(z) = f_3'(z) + i\nu f_3(z) \ ;$$

we map the z -plane onto a ζ -plane by the same conformal transformation as before; we use the methods described by Muskhelishvili (1953) to find $g_3(z(\zeta)) = G_3(\zeta)$; finally we use the definition of $g_3(z)$ as a differential equation which we solve for $f_3(z)$.

The function $G_3(\zeta)$ is found to be:

$$G_3(\zeta) = -\frac{1}{\pi}\sqrt{\frac{(\zeta^2-\alpha^2)(\zeta^2-\beta^2)}{\zeta^2-\gamma^2}}\left\{\int_\alpha^\beta \frac{(t^2-\gamma^2)\,dt}{(t-\zeta)\,|(t^2-\alpha^2)(\beta^2-t^2)|^{1/2}} + \int_{-\beta}^{-\alpha} \frac{(t^2-\gamma^2)\,dt}{(t-\zeta)\,|(t^2-\alpha^2)(\beta^2-t^2)|^{1/2}}\right\} \quad (36)$$

$$= -\frac{2\zeta}{\pi}\sqrt{\frac{(\zeta^2-\alpha^2)(\zeta^2-\beta^2)}{\zeta^2-\gamma^2}}\int_\alpha^\beta \frac{(t^2-\gamma^2)\,dt}{(t^2-\zeta^2)\,|(t^2-\alpha^2)(\beta^2-t^2)|^{1/2}} .$$

The Plemelj formulas may be used to show that this function satisfies the necessary conditions: $Re\{G_3\} = \pm 1$ on the right and left barriers, respectively, $Im\{G_3\} = 0$ on the undisturbed surface, and $Re\{G_3\} = 0$ on the vertical axis.

The solution of the differential equation gives us:

$$f_3(z) = F_3(\zeta) = e^{-i\nu z(\zeta)}\left\{\int_0^\zeta e^{i\nu z(t)}\,\frac{dz}{dt}\,G_3(t)\,dt + K_3\right\} , \quad (37)$$

where the complex constant K_3, is found from conditions (34) and (35') to be:

$$K_3 = (\sin \nu a)^{-1}\left[(1/\nu) - \int_0^\alpha \sin \nu[a-x(t)]\,\frac{dz}{dt}\,G_3(t)\,dt\right] . \quad (38)$$

This is a purely real number, just as was K_2.

At great distances from the barriers, we can derive the following asymptotic estimates:

$$Re\{f_3(z)\} \sim e^{\nu y}\,[A_3 \cos \nu x \pm B_3 \sin \nu x] \text{ , as } x \to \pm\infty , \quad (39)$$

where

$$A_3 = D_3 \cos \nu a + E_3 + K_3 , \quad (39a)$$

$$B_3 = D_3 \sin \nu a \ , \tag{39b}$$

$$D_3 = -\int_{\alpha-i0}^{\beta-i0} dt \, \frac{dz}{dt}[G_3(t) - 1][e^{\nu y(t)} - e^{-\nu y(t)}] \ , \tag{39d}$$

$$E_3 = \int_0^{i\infty} dt \, \frac{dz}{dt} \, G_2(t) \, e^{-\nu y(t)} \ . \tag{39e}$$

The velocity potential and the free-surface disturbance are given by:

$$\phi(x,y,t) = Re\{f_3(z)\} \cdot \begin{Vmatrix} M \cos \omega t \\ N \sin \omega t \end{Vmatrix} \ , \tag{40}$$

$$\eta(x,t) = (\omega/g) \, Re\{f_3(x-i0)\} \cdot \begin{Vmatrix} M \sin \omega t \\ -N \cos \omega t \end{Vmatrix} \ , \tag{41}$$

where M and N are arbitrary real constants.

(4) Antisymmetrical standing waves in presence of barriers

For a problem with symmetrical geometry, such as we are considering here, it can be shown that any solution can be represented as the sum of an even part and an odd part. In problem (3), we found a solution in which the wave elevation and the velocity potential are even in x, and the stream function is odd in x. Now we find the solution in which the wave elevation and velocity potential are odd, the stream function even. As in problem (3), there is no applied pressure field, and so the problem is linear and homogeneous.

The free-surface condition is again:

$$\phi_y - \nu\phi = 0 \ , \qquad y = 0 \ , \qquad -\infty < x < \infty \ .$$

On the axis of symmetry, we set:

$$\phi = 0 , \qquad x = 0 , \qquad y < 0 . \tag{42}$$

On the barriers, the stream function is again a constant, of course. Since ψ is even in x, the constant is the same on both barriers, and we choose the following convenient value:

$$\psi = -1/\nu , \qquad x = \pm a , \quad -b < y < 0 . \tag{43}$$

The steps all proceed just as before. We use the definitions of problem (3), replacing the subscript 3 by 4. The solution is:

$$G_4(\zeta) = \frac{1}{\pi} \frac{\sqrt{(\zeta^2-\alpha^2)(\zeta^2-\beta^2)}}{\zeta^2-\gamma^2} \left(\int_{\alpha}^{\beta} + \int_{-\beta}^{-\alpha} \right) \frac{(t^2-\gamma^2)\,dt}{(t-\zeta)\,|(t^2-\alpha^2)(\beta^2-t^2)|^{1/2}} .$$

We can integrate this solution or we can use the method explained in Appendix A to show that a much simpler representation is possible:

$$G_4(\zeta) = 1 - \frac{d\zeta}{dz} . \tag{44}$$

The solution for the complex potential, $f_4(z)$, is then:

$$f_4(z) = e^{-i\nu z} \left\{ \int_0^{\zeta} e^{i\nu z(t)} \left[\frac{dz}{dt} - 1 \right] dt + iK_4 \right\} , \tag{45}$$

where K_4 is given by:

$$K_4 = -1/\nu - (\cos \nu a)^{-1} \int_0^{\alpha} \sin \nu[a-x(t)]\,dt . \tag{46}$$

The asymptotic form of the solution is:

$$Re\{f_4(z)\} \sim e^{\nu y} \left[\pm A_4 \cos \nu x + B_4 \sin \nu x\right] , \tag{47}$$

where

$$A_4 = D_4 \cos \nu a , \tag{47a}$$

$$B_4 = D_4 \sin \nu a + E_4 + K_4 + 1/\nu , \tag{47b}$$

$$D_4 = - \int_{\alpha-i0}^{\beta-i0} dt \left[e^{\nu y(t)} - e^{-\nu y(t)}\right] , \tag{47d}$$

$$E_4 = - \int_0^{\infty} dt\, e^{-\nu y(it)} . \tag{47e}$$

The velocity potential and the free-surface disturbance are given by the same expressions as in the previous problem if f_3 be replaced by f_4 .

WAVEMAKER WITH A LIP

We now consider the wavemaker problem in which a sinusoidally varying, uniform pressure is applied to the part of the free surface between the barriers. Actually, a rigid wall is assumed to be located at the y -axis, and so we admit only solutions for which ψ is constant on the vertical axis. The solutions of problems (2) and (3) satisfy this condition, and all we need to do is superpose these solutions in such a way that the radiation condition is satisfied, that is, that the sum represents outgoing waves as $x \to \pm\infty$.

Let the solution be:

$$\phi(x,y,t) = Re\{f_2(z)\} \cos \omega t + M\, Re\{f_3(z)\} \cos \omega t + N\, Re\{f_3(z)\} \sin \omega t .$$

We use the asymptotic expressions given in (31) and (39), and we find then that the solution has the proper form only if:

$$M = -\frac{A_2A_3 + B_2B_3}{A_3^2 + B_3^2} ;$$

$$N = \frac{-A_3B_2 + A_2B_3}{A_3^2 + B_3^2} .$$

The asymptotic form of $\phi(x,y,t)$ is then:

$$\phi(x,y,t) \sim \frac{A_2B_3 - A_3B_2}{A_3^2 + B_3^2} e^{\nu y}\left[B_3 \cos(\omega t \mp \nu x) + A_3 \sin(\omega t \mp \nu x) \right],$$

and the amplitude of the generated waves is:

$$h = \frac{\omega}{g} \frac{|A_2B_3 - A_3B_2|}{A_3^2 + B_3^2} .$$

In Figure 7, the wave amplitude, h, is plotted against $\nu a = 2\pi a/\lambda$, where λ is the wavelength; the ratio of lip immersion to wavemaker width, b/a, is a parameter. The curve for $b/a = 0$ is a graph of the function $|\sin \nu a|$; from Equation (9), this is the wave amplitude (non-dimensionalized) from the Stoker model of the wavemaker, in which the lip is not represented.

Stoker pointed out the interesting fact that the theory predicts no radiated waves if νa is an integer multiple of π. The same fact is clearly true for any value of b/a, although our formulas are indeterminate under these conditions.

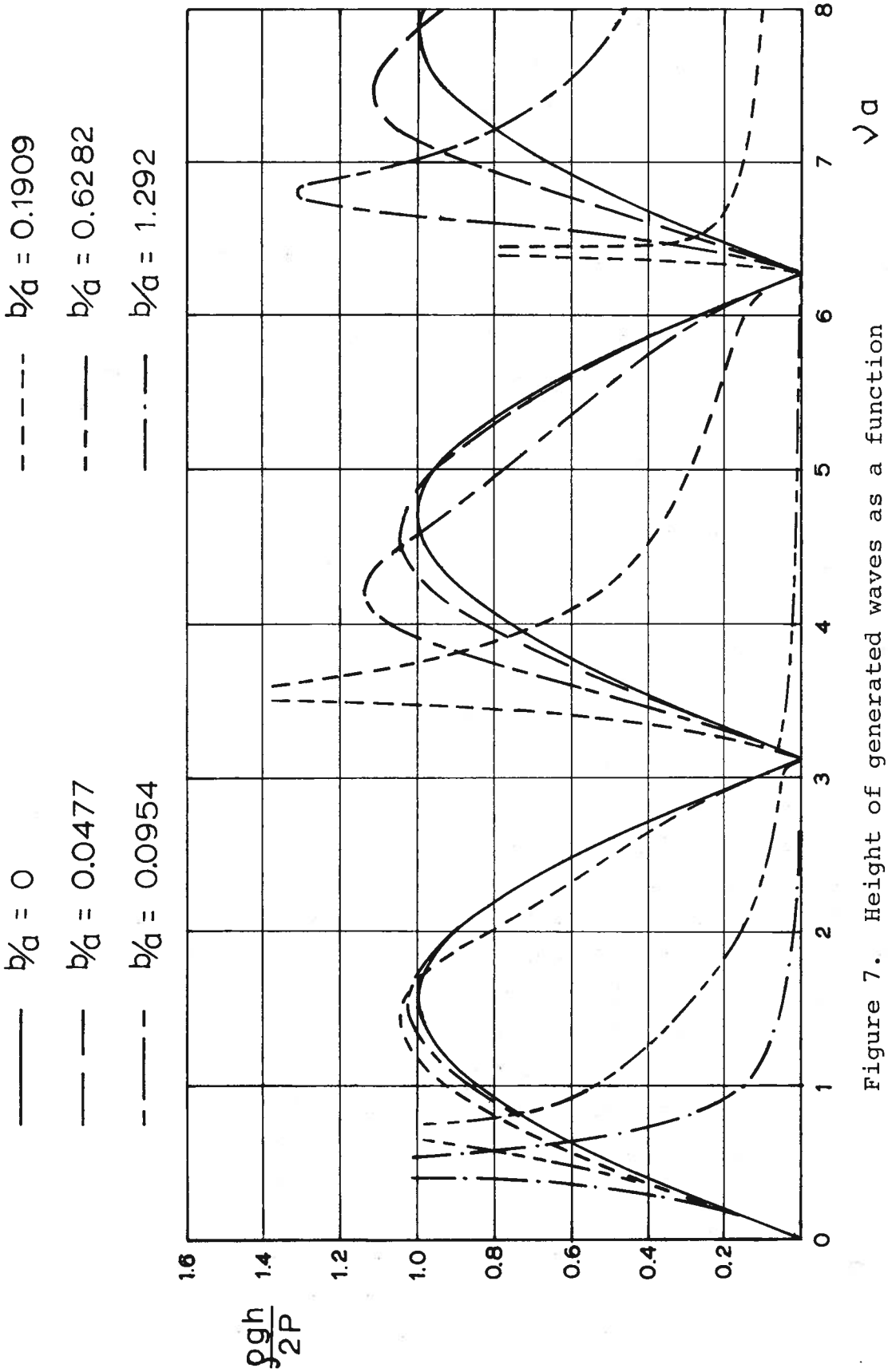

Figure 7. Height of generated waves as a function of $\sqrt{a}$, for various values of lip immersion.

For $\nu a < \pi$, the curve for the case $b/a = 0.0477$ cannot be distinguished from the sine curve which corresponds to $b/a = 0$. However, for larger ranges of νa , the curves are distinctly different, and the difference increases in the following humps. The very small lip, corresponding to $b/a \simeq 1/20$, apparently magnifies the amplitude of short waves which are generated. It may also be noticed that the humps in the response curve for $b/a = 0.0477$ become succesively more skewed. It is not unreasonable to suppose that these humps farther out to the right eventually take on the appearance of the humps at the left for larger values of b/a .

For long waves ($\nu a \to 0$), the effect of the lip in amplifying the waves is quite evident with the larger values of b/a . We did not consider it worth the computer time to try to obtain enough points to fill in all of these curves. Under the conditions of violent motion that must prevail near these peaks, it is, in fact, somewhat difficult to take the theory seriously at all. However, the trends are quite clear from Figure 7.

In Figure 8, the effect of the lip is shown in a different way. For a given frequency (or wavelength) of generated wave, the influence of lip size on wave amplitude is quite apparent here. For each wavelength, the amplitude at the left is the no-lip value; in each case, the amplitude increases and then decreases. Note however that we have included only the longer waves in this figure. The largest value of νa is 1.50 , corresponding to a wavelength $\lambda \simeq 4.2a$. This restriction was made because it seems to include the practical range of wavelengths that one would try to generate with a pneumatic wavemaker.

In using these calculations, it would be desirable to be able to predict the immersion of the lip which is necessary if the wavemaker is to produce waves of specified wave-

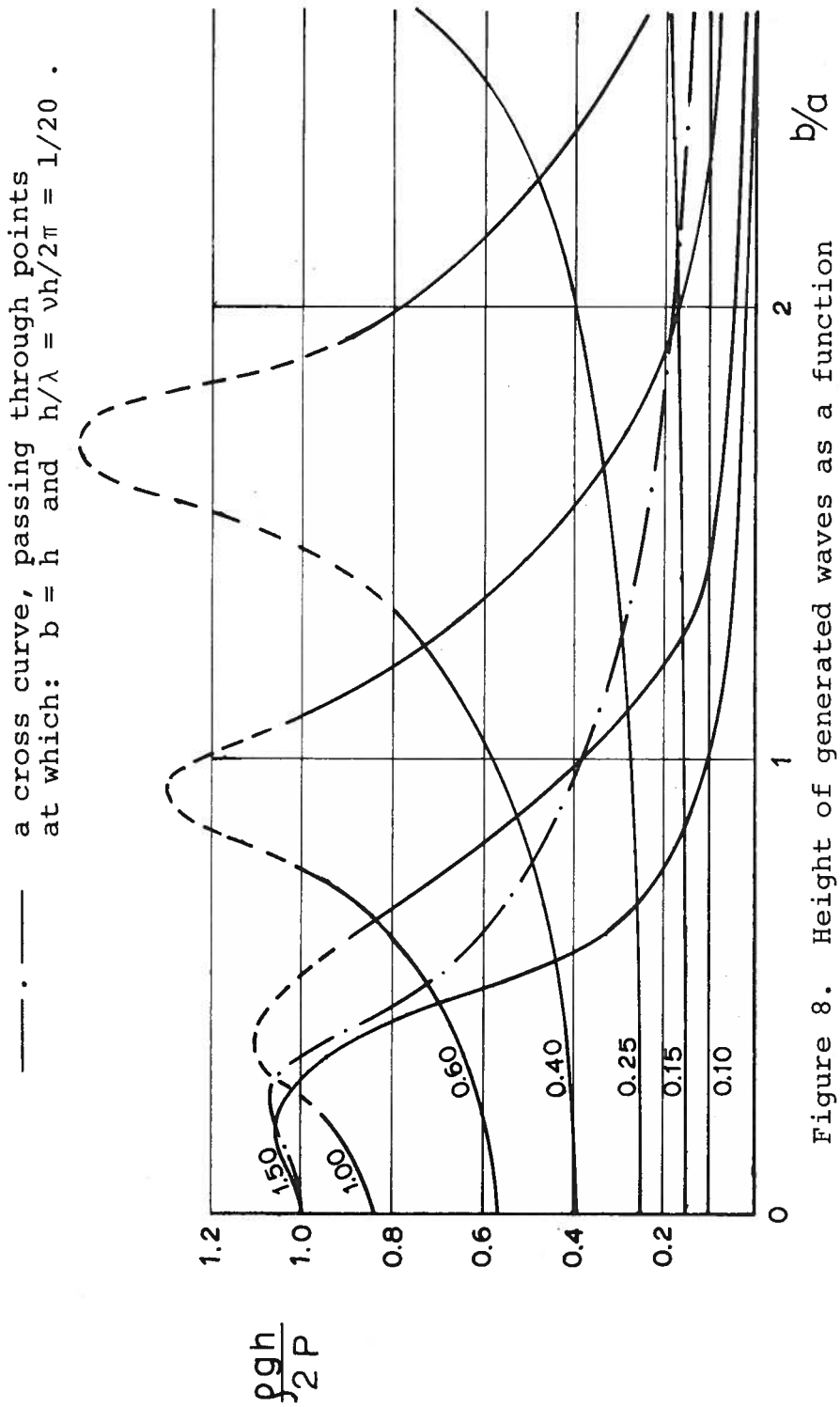

Figure 8. Height of generated waves as a function of lip immersion, for various values of νa .

length and amplitude. This is not a straightforward matter at all, however, for the analysis is based on linearized water-wave theory, which implies, among other things, that all physical dimensions in the problem, including lip immersion, must be *large* compared with wave amplitude. In practice, we may expect that the lip immersion should be at least equal to the wave amplitude; such an estimate is probably a lower bound on lip size. In Figure 8, an extra curve is shown which passes through the other curves at the points at which $b = h$ for a wave amplitude equal to 1/20 of the wavelength. Thus, for $\nu a = 0.15$, the wavelength is $2\pi a/0.15 \simeq 42a$ — a very long wave indeed. If this wave has amplitude/length ratio of 1/20, the amplitude will be about $2.1a$, and this gives a lower limit on b/a of 2.1. It should be noted that the "amplitude" here is a single amplitude, that is, half of the crest-to-trough distance, and so a 1/20 amplitude-to-wavelength ratio is exceedingly large.

Although it may not be possible to use these results quantitatively for deciding upon lip immersion, Figure 8 does show the way in which lip size must be increased in order to produce longer and longer waves of constant maximum slope. What is perhaps more important is the following: If the lip size is chosen so that large amplitude long waves can be produced, then it will be practically impossible to produce short waves. Some compromise is clearly necessary. Only experiments can show what is the best compromise.

WAVES INCIDENT ON TWO BARRIERS

Let there be incident waves from the left having unit amplitude and frequency ω. Once again, we have the two barriers shown in Figure 4. In order to find the velocity potential valid throughout the fluid, we need only to combine the symmetric and antisymmetric solutions of problem (3) and

(4). Thus, let:

$$\phi(x,y,t) = P\ Re\{f_3(z)\} \cos \omega t + Q\ Re\{f_4(z)\} \cos \omega t$$

$$+ R\ Re\{f_3(z)\} \sin \omega t + S\ Re\{f_4(z)\} \sin \omega t\ .$$

We use the asymptotic estimates of $f_3(z)$ and $f_4(z)$ from (39) and (47) :

$$Re\{f_3(z)\} \sim e^{\nu y}\ [A_3 \cos \nu x \pm B_3 \sin \nu x]$$

$$Re\{f_4(z)\} \sim e^{\nu y}\ [\pm A_4 \cos \nu x + B_4 \sin \nu x] \qquad \text{as} \quad x \to \pm \infty\ .$$

When these estimates are substituted into the assumed expression for the velocity potential, the result should represent: (1) the incident wave (of unit amplitude) plus a reflected wave, as $x \to -\infty$; (2) a transmitted wave, as $x \to +\infty$.

If we now set:

$$(\omega/g)\ P = A_3/(A_3^2+B_3^2)\ ; \qquad (\omega/g)\ R = -B_3/(A_3^2+B_3^2)\ ;$$

$$(\omega/g)\ Q = -A_4/(A_4^2+B_4^2)\ ; \qquad (\omega/g)\ S = B_4/(A_4^2+B_4^2)\ ,$$

the wave disturbance at infinity is given by:

$$\eta(x,t) \sim \sin(\omega t-\nu x) + \sin(\omega t+\nu x) \left[\frac{1}{2} \left(\frac{A_3^2-B_3^2}{A_3^2+B_3^2} + \frac{A_4^2-B_4^2}{A_4^2+B_4^2} \right) \right]$$

$$+ \cos\ (\omega t+\nu x) \left[\frac{A_3 B_3}{A_3^2 + B_3^2} + \frac{A_4 B_4}{A_4^2 + B_4^2} \right]\ , \quad x \to -\infty\ ;$$

$$\eta(x,t) \sim \sin(\omega t-\nu x)\left[\frac{1}{2}\left(\frac{A_3^2-B_3^2}{A_3^2+B_3^2} + \frac{A_4^2-B_4^2}{A_4^2+B_4^2}\right)\right]$$

$$+ \cos(\omega t-\nu x)\left[\frac{A_3B_3}{A_3^2+B_3^2} - \frac{A_4B_4}{A_4^2+B_4^2}\right] , \quad x \to +\infty .$$

This result clearly satisfies the requirements set.

Since the incident wave has unit amplitude, we can define the reflection coefficient as the magnitude of the reflected wave, R, given by:

$$R = \left[\frac{(A_3A_4 + B_3B_4)^2}{(A_3^2+B_3^2)(A_4^2+B_4^2)}\right]^{1/2} .$$

Similarly, the transmission coefficient, T, is given by the amplitude of the transmitted wave:

$$T = \left[\frac{(A_3B_4 - A_4B_3)^2}{(A_3^2+B_3^2)(A_4^2+B_4^2)}\right]^{1/2} .$$

A simple algebraic check shows that $T^2 + R^2 = 1$.

FORCE ON AN OSCILLATING INVERTED BOX

This problem is really just a slight variation on the wavemaker problem: let the oscillating pressure be caused by the heave motion of an inverted box, as shown in Figure 9. Assume that the base of the box is at a height:

$$h(t) = h_0 + H\cos(\omega t + \varepsilon) . \qquad (48)$$

The sidewalls of the box extend downwards sufficiently far so that their edges are always immersed. The only ad-

ditional problem here is to find the relation between $h(t)$ and $p(t)$, the pressure applied to the free surface.

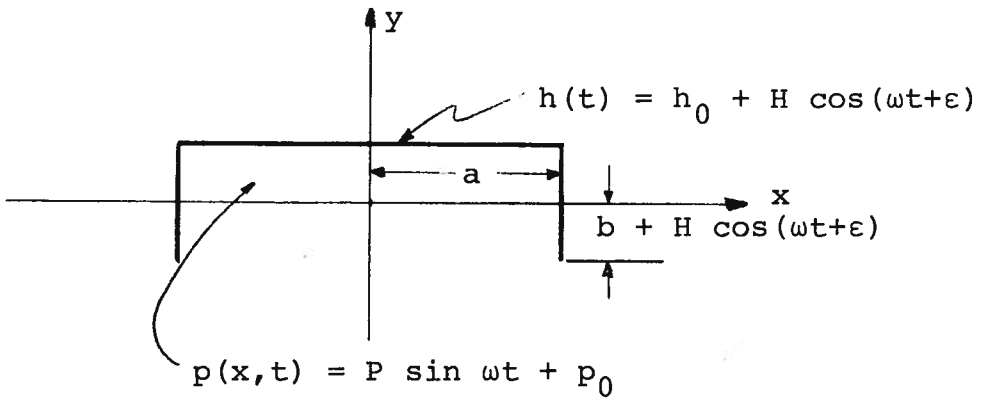

Figure 9

We shall ignore the hydrodynamic effects of the box sides, other than assuming that the sides provide a physical boundary on the region of the oscillating applied pressure. Under this assumption, the problem reduces to the previous problem (1) (Stoker's problem). If we knew the pressure under the box, we could immediately write down the complete solution of the linearized free-surface problem. Most of our effort goes into relating the motion of the box with the amplitude and phase of the applied pressure.

The free-surface conditions are:

$$\frac{p}{\rho} + \phi_t + g\eta = \frac{p_{atm}}{\rho} \quad , \quad y = 0 \; ;$$

$$\phi_y - \eta_t = 0 \; , \qquad y = 0 \; .$$

For $|x| > a$, $p = p_{atm}$ = atmospheric pressure. For $|x| < a$, we shall assume that the pressure is given by the adiabatic gas law, and so we must calculate the volume of air enclosed between the box and the free surface. For $|x| < a$, let:

$$\eta_0 = - \frac{p_0 - p_{atm}}{\rho g} \quad , \tag{49}$$

$$\overline{\eta} \cos(\omega t+\delta) = (1/2a) \int_{-a}^{+a} [\eta(x,t) - \eta_0] \, dx \quad , \tag{50}$$

where p_0 is the static pressure under the box. Clearly, η_0 gives the static depression of the free surface, and $\overline{\eta} \cos(\omega t+\delta)$ gives the space average of the oscillatory depression of the free surface. By the adiabatic gas law, the pressure varies inversely with the volume raised to the γ power, where $\gamma = 1.4$ for air. We can write the adiabatic gas law as follows:

$$p = p_0 \left[\frac{h_0 - \eta_0}{h_0 - \eta_0 + H \cos(\omega t+\varepsilon) - \overline{\eta} \cos(\omega t+\delta)} \right]^{\gamma}$$

$$= p_0 \left[1 + \frac{H}{h_0-\eta_0} \cos(\omega t+\varepsilon) - \frac{\overline{\eta}}{h_0-\eta_0} \cos(\omega t+\delta) \right]^{-\gamma} .$$

Since we assume that the problem can be linearized in all other aspects, we may as well assume here that the oscillations have small amplitude, in which case the last equation can be approximated by:

$$p \simeq p_0 \left[1 - \frac{\gamma}{h_0-\eta_0} \left[H \cos(\omega t+\varepsilon) - \overline{\eta} \cos(\omega t+\delta) \right] \right] .$$

Let us now define the oscillatory pressure in a way which suggests immediately how the problem reduces to the previous problem (1):

$$P \sin \omega t \equiv p - p_0$$

$$= - \frac{\gamma p_0}{h_0 - \eta_0} \left[H \cos(\omega t + \varepsilon) - \bar{\eta} \cos(\omega t + \delta) \right] \quad . \quad (51)$$

Thus, the problem is actually identical to problem (1), except that we cannot simply specify P. We shall have to relate P to the parameters which describe the motion of the box, viz., to H and ε.

The procedure is as follows:

(a) Solve problem (1) for arbitrary P.

(b) Calculate $\bar{\eta}$, δ, as functions of P.

(c) Find H, ε from the gas law, as functions of P, γ, p_0, h_0, etc.

(d) The oscillatory force on the box is $2aP \sin \omega t$. With H and ε known as functions of P, the force can be related directly to the amplitude and phase of the box motion.

(a) The solution of problem (1) has already been given. The particular quantities we need are (from (10) and (7)):

$$\eta(x,t) - \eta_0 = \left[-\frac{P}{\rho g} (1 + 2\sin \nu a \sin \nu x) + \frac{\omega}{g} Re\{f(x-i0)\} \right] \sin \omega t + \left[\frac{2P}{\rho g} \sin \nu a \cos \nu x \right] \cos \omega t \quad , \quad \text{for } |x| < a \ ;$$

$$f(z) = - \frac{\omega P}{\pi \rho g} e^{-i\nu z} \int_{C_{i\infty}}^{z} dt \, e^{i\nu t} \log \frac{t-a}{t+a} \ ,$$

with the contour of the integral as specified previously.

(b) Let $g(x)$ be the standard function:

$$g(x) \equiv \int_0^\infty \frac{u \, e^{-xu} du}{u^2 + 1} \ ,$$

This function is frequently used in treating sine and cosine integrals (See Abramowitz and Stegun (1964), 5.2.13). It has the great virtue that it can be computed very easily. In Appendix B, we show that the mean oscillatory water elevation under the box is given at any instant by:

$$\bar{\eta}\ \cos(\omega t+\delta) = \frac{2P}{\rho g \nu a}\left[\ \sin^2\nu a\ \cos\ \omega t \right. \tag{52}$$
$$\left. + \frac{1}{2\pi}\ [-2\pi\ \sin\nu a\ \cos\nu a + C + \log\ 2\nu a + g(2\nu a)]\sin\omega t\right] .$$

Here, the constant C is the Euler constant, $C = 0.577216$. (C is usually denoted by γ in modern literature, but we reserve the latter for the specific-heat ratio.)

(c) From the definition of P , Equation (51), we solve for $H\cos(\omega t+\varepsilon)$:

$$H\cos(\omega t+\varepsilon) = -\frac{h_0-\eta_0}{p_0\gamma}\ P\ \sin\ \omega t + \bar{\eta}\ \cos(\omega t+\delta)$$
$$= \sin\ \omega t\left[-\frac{h_0-\eta_0}{p_0\gamma} + \frac{1}{\pi\rho g\nu a}[-2\pi\ \sin\nu a\ \cos\nu a\right.$$
$$\left. + C + \log\ 2\nu a + g(2\nu a)]\right]$$
$$+ \cos\ \omega t\left[\frac{2}{\rho g\nu a}\ \sin^2\nu a\right] .$$

We can also write this quantity as follows:

$$H\cos(\omega t+\varepsilon) = H\ [\cos\ \varepsilon\ \cos\ \omega t - \sin\ \varepsilon\ \sin\ \omega t\ ] .$$

Thus we can solve for H and ε from the following relations:

$$\frac{H}{P}\ \cos\ \varepsilon = \frac{2\ \sin^2\nu a}{\rho g\nu a}\ ; \tag{53a}$$

$$\frac{H}{P} \sin \varepsilon = \frac{h_0 - \eta_0}{p_0 \gamma} + \frac{1}{\pi \rho g \nu a} [2\pi \sin \nu a \cos \nu a - C - \log 2\nu a - g(2\nu a)] \; . \tag{53b}$$

(d) First, let us observe the following:

$$\text{Height of box base} = H \cos(\omega t + \varepsilon) + h_0 \; ;$$

$$\text{Velocity of box} = -\omega H \sin(\omega t + \varepsilon) \; ;$$

$$\text{Acceleration of box} = -\omega^2 H \cos(\omega t + \varepsilon) \; .$$

We assume that the oscillatory force on the box base can be written as the sum of inertial, damping, and restoring-force components:

$$\begin{aligned} \text{Oscillatory force} &= - m[-\omega^2 H \cos(\omega t + \varepsilon)] \\ &\quad - N[-\omega H \sin(\omega t + \varepsilon)] \\ &\quad - c[H \cos(\omega t + \varepsilon)] \end{aligned}$$

$$\begin{aligned} &= \cos \omega t \; [m\omega^2 H \cos \varepsilon + N\omega H \sin \varepsilon - cH \cos \varepsilon] \\ &\quad + \sin \omega t \; [-m\omega^2 H \sin \varepsilon + N\omega \cos \varepsilon + cH \sin \varepsilon] \; . \end{aligned}$$

But the oscillatory force can also be written: $2aP \sin \omega t$. Equating these two formulas for the force, we can solve for the coefficients:

$$m\omega^2 - c = - \frac{2a}{(H/P)^2} \frac{H}{P} \sin \varepsilon \; ; \tag{54}$$

$$\omega N = \frac{2a}{(H/P)^2} \frac{H}{P} \cos \varepsilon \; . \tag{55}$$

In the usual language of ship-motion theory, m is the added mass, N is the damping coefficient, and c is the restoring-force coefficient, all expressed per unit length of ship.

In order to define m and c uniquely, we must make another arbitrary definition. We shall assume that c is the restoring-force coefficient which would be applicable if the water responded only statically to the applied oscillatory pressure. If this were the case, we would have the following equivalents of steps (a), (b), and (c):

(a') $\eta(x,t) - \eta_0 = -(P/\rho g) \sin \omega t$,

(b') $\bar{\eta} \cos(\omega t+\delta) = -(P/\rho g) \sin \omega t$.

(c') $$H \cos(\omega t+\varepsilon) = -\left[\frac{h_0-\eta_0}{p_0\gamma} + \frac{1}{\rho g}\right] P \sin \omega t \ .$$

Combining these, we obtain:

$$\left.\begin{aligned} \frac{H}{P} \cos \varepsilon &= 0 \\ \frac{H}{P} \sin \varepsilon &= \frac{h_0-\eta_0}{p_0\gamma} + \frac{1}{\rho g} \end{aligned}\right\} \text{ for static responses.}$$

(d') Oscillatory force $= 2aP \sin \omega t = - c H \cos(\omega t+\varepsilon)$

$$= c H \sin \varepsilon \sin \omega t \ ,$$

since $\cos \varepsilon = 0$. Now H , P , and c are all positive constants, and so $\sin \varepsilon = +1$, which implies that $\varepsilon = \pi/2$. Thus,

$$c = 2aP/H = \frac{2a}{\frac{h_0-\eta_0}{p_0\gamma} + \frac{1}{\rho g}} \quad . \tag{56}$$

Now we can return to the dynamics problem, using the above value of c in the expression for $(m\omega^2-c)$ to yield a unique value for the added-mass coefficient:

$$m = \frac{2a^2\rho}{\nu a\left[1 + \frac{\rho g(h_0-\eta_0)}{p_0\gamma}\right]} - \frac{2a}{g\nu(H/P)^2}\,\frac{H}{P}\sin\varepsilon \quad . \tag{57}$$

The quantities H/P and $(H/P)\sin\varepsilon$ must be computed from Equations (53). It is easily checked now that all quantities in the expressions for m and N are known.

Since the neglect of the sidewalls is probably justified only for long waves (low frequencies), it is worthwhile to obtain simplified formulas for m and N which are valid asymptotically as $\omega \to 0$. The results are:

$$N \sim \frac{4\rho a^2\omega}{\left[1 + \frac{\rho g(h_0-\eta_0)}{p_0\gamma}\right]^2} \quad , \qquad \text{as} \quad \omega \to 0 \ .$$

$$m \sim \frac{2\rho a^2[3 - 2(C + \log 2\nu a)]}{\pi\left[1 + \frac{\rho g(h_0-\eta_0)}{p_0\gamma}\right]} \quad ,$$

Figures 10 and 11 show how m and N vary with a, for various constant values of the parameter $\rho g(h_0-\eta_0)/p_0\gamma$. The latter is dependent only on the static conditions of operation. As $\nu a \to 0$, the added mass, m, approaches infinity logarithmically, and the damping coefficient, N, approaches zero linearly with ω.

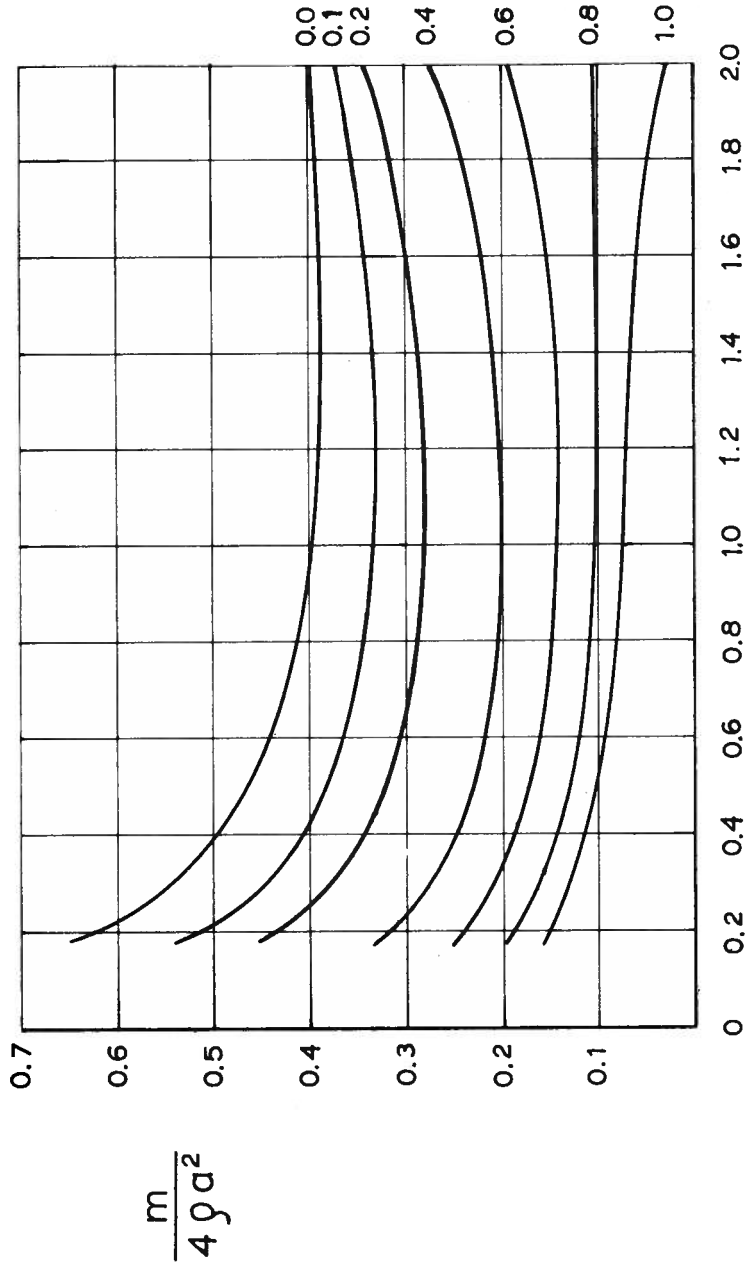

Figure 10. Added mass coefficient as a function of νa, for various values of $\rho g(h_0-\eta_0)/p_0\gamma$.

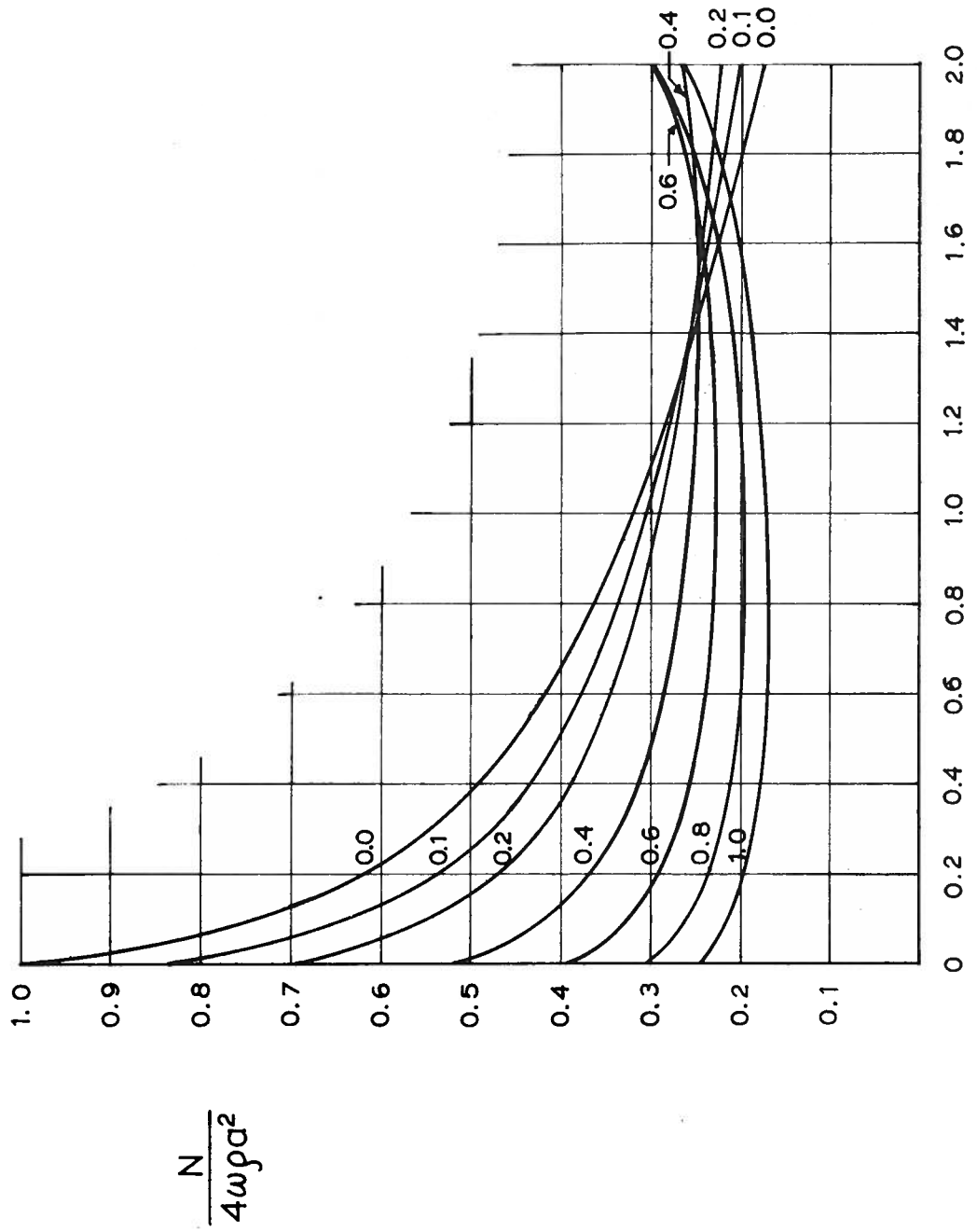

Figure 11. Damping coefficient as a function of νa, for various values of $\rho g(h_0-\eta_0)/p_0\gamma$.

There is nothing startling about these results. If the box is very close to the water surface, so that the enclosed volume of air is relatively small, the added-mass and the damping coefficients are large, at least for low to moderate frequencies. It should be noted, incidentally, that the calculation for the case $\rho g(h_0-\eta_0)/p_0\gamma = 0$ is really meaningless, since we earlier assumed that $h_0-\eta_0$ was large compared with the amplitude of oscillation of the box and of the free surface.

In evaluating the motions behavior of the box, it may well turn out that the most important effect to be considered is the difference in the restoring-force coefficient, in comparision with that of a solid body. If $h_0-\eta_0$ is zero, the restoring-force coefficient is $c = 2a\rho g$, the same value that one obtains for a solid body of beam $2a$. From Equation (56) it can be seen that the actual value of c is always less than $2a\rho g$.

REFERENCES

Abramowitz, A. , and Stegun, I. A., *Handbook of Mathematical Functions*. National Bureau of Standards, Applied Mathematics Series - 55. U.S. Govt. Printing Office, Washington, D. C. (1964)

Levine, H., and Rodemich, E., *Scattering of Surface Waves on an Ideal Fluid*. Tech. Report No. 78, Applied Math. & Stat. Lab., Stanford University. (1958)

Muskhelishvili, N. I., *Singular Integral Equations*. P. Noordhoff, Groningen. (1953)

Stoker, J. J., *Water Waves*. Interscience, New York. (1957)

Wehausen, J. V., and Laitone, E. V., "Surface Waves," *Encyclopedia of Physics*, Vol. IX. Springer-Verlag, Berlin. (1960)

Appendix A

The Conformal Mapping

The conformal mapping given in Equation (23) has the following properties:

(a) There is no magnification of the scale at infinity.

(b) The origins in the two planes are images of each other.

(c) The real axis in the ζ -plane (for $\eta = -0$) corresponds to a contour in the z -plane along the undisturbed free surface and around the under sides of the barriers. Se Figure 5.

From Figure 5, it is obvious that:

$$z_H - z_F = i\int_\alpha^\beta \frac{(t^2-\gamma^2)\,dt}{|(t^2-\alpha^2)(\beta^2-t^2)|^{1/2}} = 0 \ .$$

Therefore, the constant γ is given by:

$$\gamma^2 = \int_\alpha^\beta \frac{t^2 dt}{|(t^2-\alpha^2)(\beta^2-t^2)|^{1/2}} \Bigg/ \int_\alpha^\beta \frac{dt}{|(t^2-\alpha^2)(\beta^2-t^2)|^{1/2}} \ .$$

Then a and b can be found in terms of α and β :

$$a = \int_0^\alpha \frac{(\gamma^2-t^2)\,dt}{|(\alpha^2-t^2)(\beta^2-t^2)|^{1/2}} \ ;$$

$$b = \int_\alpha^\gamma \frac{(\gamma^2-t^2)\,dt}{|(t^2-\alpha^2)(\beta^2-t^2)|^{1/2}} \ .$$

The procedure used in the numerical analysis was to choose α and β arbitrarily, then find γ , a , and b . (This accounts for the rather odd values of b/a .)

A fact which is used several times in the text (in finding asymptotic estimates at infinity) is the following:

$$z(\zeta) - \zeta = \mathcal{O}(1/\zeta) \quad \text{as} \quad \zeta \to \infty \ .$$

The proof is as follows:

From Equation (23), we can write:

$$z(\zeta) - \zeta = \int_0^{\zeta} \left[\frac{t^2-\gamma^2}{\sqrt{(t^2-\alpha^2)(t^2-\beta^2)}} - 1 \right] dt \ .$$

The integrand is single-valued for $|t| > \beta$, and so it can be expanded in a Laurent series about $t = 0$. We find then that the integrand is $O(1/t^2)$ as $t \to \infty$, and so $\lim_{\zeta \to i\infty} [z(\zeta) - \zeta]$ exists if we take a path along, say, the upper imaginary axis. Furthermore, we could evaluate the limit for, say, $\zeta \to \infty \cdot e^{i\theta}$ by following the same contour along the upper imaginary axis and then following a circular-arc contour from $\arg \zeta = \pi/2$ to $\arg \zeta = \theta$; as the radius of this arc approaches infinity, the contribution to the integral from the arc approaches zero. Therefore,

$$\lim_{\zeta \to \infty e^{i\theta}} [z(\zeta) - \zeta] \quad \text{exists and is independent of} \quad \theta \ .$$

Finally, calculate this limit for $\arg \zeta = -\pi/2$ by following the contour indicated in Figure 12. The part along the real axis contributes nothing. (γ was chosen to make this so.) Then,

$$\lim_{\zeta \to -i\infty} [z(\zeta) - \zeta] = \int_0^{-i\infty} \left[\frac{t^2-\gamma^2}{\sqrt{(t^2-\alpha^2)(t^2-\beta^2)}} - 1 \right] dt$$

$$= - \int_0^{i\infty} \left[\frac{t^2-\gamma^2}{\sqrt{(t^2-\alpha^2)(t^2-\beta^2)}} - 1 \right] dt$$

(by a change of variable)

$$= - \lim_{\zeta \to i\infty} [z(\zeta) - \zeta] .$$

However, the limit at the start of this calculation is also equal to the limit at the end, since the limit does not depend on θ . Therefore, the limit is zero.

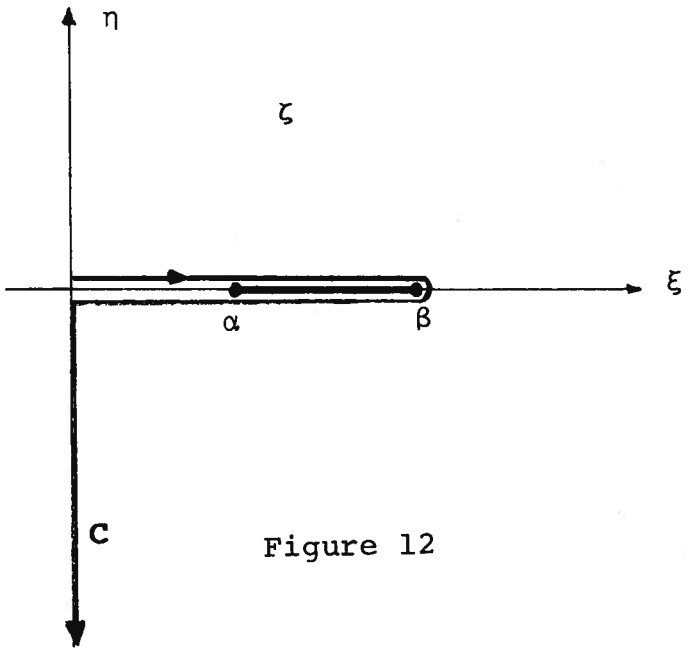

Figure 12

We can now also write $z(\zeta)$ in the following way:

$$z(\zeta) = \zeta + \int_\infty^\zeta \left[\frac{t^2-\gamma^2}{\sqrt{(t^2-\alpha^2)(t^2-\beta^2)}} - 1 \right] dt .$$

Since the integrand is $O(1/t^2)$, the integral is $O(1/\zeta)$, which was to be proven.

In problem (4), a particularly simple solution was found, as given by Equation (44). This solution can be obtained by a very tedious integration of the solution which results from using the methods of Muskhelishvili, but the following proof of equivalence is much easier:

The quantity:

$$\frac{dz}{d\zeta}\,[G_4(\zeta) - 1]$$

is single-valued on the two cuts in the ζ-plane. It is thus analytic in the whole plane except possibly at the ends of the cuts. But at these ends it is less singular than a simple pole. Therefore these singularities are removable, and the function is analytic in the whole plane. The quantity is bounded at infinity, and so it must be a constant. The value of the constant may be found by evaluating the quantity as $\zeta \to \infty$, and we find that:

$$\frac{dz}{d\zeta}\,[G_4(\zeta) - 1] = -1 .$$

This shows the equivalence of the two solutions.

It is interesting to note that the quantity

$$\frac{dz}{d\zeta}\,[G_3(\zeta) - 1]$$

is analytic in the neighborhood of the right-hand cut in the ζ-plane, but not on the left-hand cut.

Appendix B

Calculation of $\bar{\eta}\cos(\omega t+\delta)$

For the inverted-box problem, we need to know the average height of the water at any instant under the box. For $|x|<a$, the local surface elevation is given by (Equation (10)):

$$\eta(x,t) = \left[-\frac{P}{\rho g}\,(1 + 2\sin \nu a \sin \nu x) + \frac{\omega}{g}\,Re\{f(x-i0)\}\right]\sin \omega t + \left[\frac{2P}{\rho g}\sin \nu a \cos \nu x\right]\cos \omega t ,$$

where

$$f(x-i0) = -\frac{\omega P}{\pi \rho g}\, e^{-i\nu x}\int_{C_{i\infty}}^{x-i0} dt\, e^{i\nu t}\log\frac{t-a}{t+a} ,$$

the contour integral being taken along the path shown in Figure 3. The whole purpose of this appendix is to sketch the rather tedious calculation of the average of $\eta(x,t)$ over the interval between $x = -a$ and $x = +a$. Obviously, the trouble comes only from the integral of $f(x-i0)$.

The integral of $f(x-i0)$ can be transformed once by an integration by parts:

$$\int_{-a}^{a} dx\, f(x-i0) = \frac{P}{\pi i \rho \omega}\left(e^{-i\nu a}\int_{C_{i\infty}}^{a-i0} dt\, e^{i\nu t}\log\frac{t-a}{t+a} - e^{i\nu a}\int_{C_{i\infty}}^{-a-i0} dt\, e^{i\nu t}\log\frac{t-a}{t+a} - \int_{-a}^{a} dx\left[\log\frac{a-x}{a+x} - i\pi\right]\right).$$

The first two integrals on the right-hand side are contour integrals, taken along the standard contour. The third inte-

gral is readily evaluated; the logarithm term yields nothing, and the other term is trivial. We have now for the integral of $f(x-i0)$:

$$\int_{-a}^{a} dx\, f(x-i0) = \frac{P}{\pi i \rho \omega}\left(2\pi i a + I_1 - I_2\right) ,$$

where:

$$I_1 = e^{-i\nu a}\int_{i\infty}^{a-i0} dt\, e^{i\nu t} \log \frac{t-a}{t+a} ;$$

$$I_2 = e^{i\nu a}\int_{i\infty}^{-a-i0} dt\, e^{i\nu t} \log \frac{t-a}{t+a} .$$

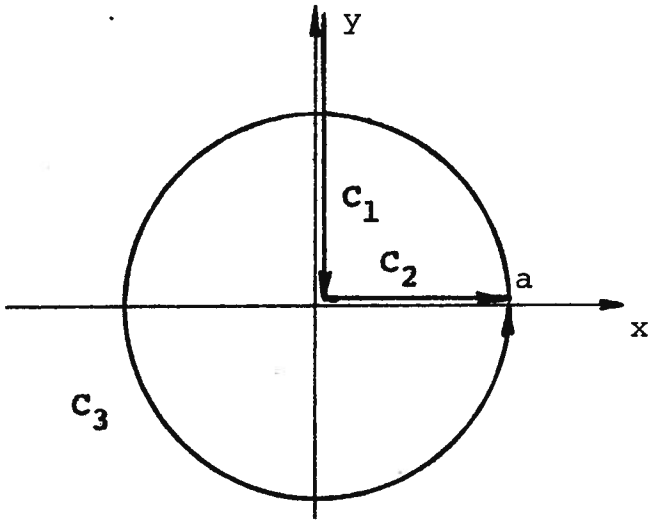

Figure 13.

The first of these, I_1 , is taken along the contour C counter-clockwise around the cut in the plane. We deform this contour into the sum of three contours, C_1 , C_2 , and C_3 , as shown in Figure 13, and we denote the respective contributions to I_1 by I_{11} , I_{12} , and I_{13} . A change of variable and a simple integration yield for the first:

$$I_{11} = \frac{1}{\nu} e^{-i\nu a} [\pi - 2 f(\nu a)] \quad ,$$

where $f(\nu a)$ is a standard function related to the sine and cosine integrals (See Abramowitz and Stegun (1964), Equation 5.2.12):

$$f(\nu a) = \int_0^\infty \frac{e^{-\nu a u}\, du}{u^2+1} \quad .$$

For the second, we can perform the following manipulations:

$$I_{12} = \int_0^a dt\, e^{-i\nu(a-t)} \left[\log \frac{a-t}{a+t} + i\pi\right]$$

$$= \frac{\pi}{\nu}(1-e^{-i\nu a}) + a\int_0^1 ds\, e^{-i\nu a s} \log s$$

$$- a\int_0^1 ds\, e^{-i\nu a(1-s)} \log(1+s)$$

$$= \frac{\pi}{\nu}(1-e^{-i\nu a}) + \frac{1}{\nu}\left[-\frac{\pi}{2} - si(\nu a) - i\, Ci(\nu a) + i(C+\log \nu a)\right]$$

$$+ \frac{1}{\nu}\Big[i \log 2 - ie^{-2i\nu a}\{Ci(2\nu a) - Ci(\nu a)$$

$$+ i\, si(2\nu a) - i\, si(\nu a)\}\Big] \quad .$$

The last equality follows from fundamental properties of the si and Ci functions. The third integral, I_{13}, can be evaluated by the method of residues after a partial integration:

$$I_{13} = - \frac{4\pi i}{\nu} e^{-i\nu a} \sin \nu a \quad .$$

The sum of the three parts is:

$$I_1 = \frac{1}{\nu} \left| \frac{\pi}{2} - si(\nu a) - i\, Ci(\nu a) + i(C + \log 2\nu a) \right.$$

$$-e^{-i\nu a} [2f(\nu a) + 4\pi i \sin \nu a]$$

$$\left. -ie^{-2i\nu a} [Ci(2\nu a) - Ci(\nu a) + i\, si(2\nu a) - i\, si(\nu a)] \right] .$$

The second integral, I_2, is broken into two parts, corresponding to the two contours C_1 and C_2 shown in Figure 14. The first of these, taken along the upper imaginary axis is quite similar to I_{11}:

$$I_{21} = \frac{1}{\nu} e^{i\nu a} [\pi - 2f(\nu a)] .$$

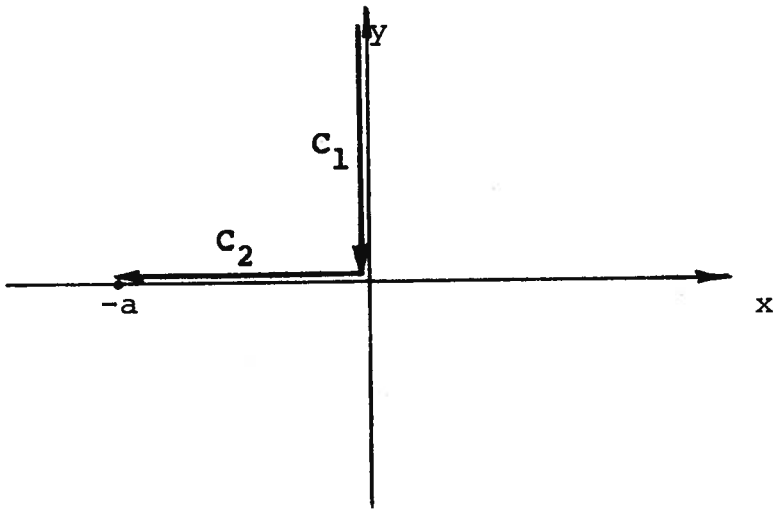

Figure 14.

The second integral, I_{22}, can be shown to be $\overline{I_{12}}$ plus an elementary function, where the bar denotes the complex conjugate of the indicated quantity. The result is:

$$I_{22} = \frac{\pi}{\nu}\,(1 - e^{i\nu a}) + \frac{1}{\nu}\Big[-\frac{\pi}{2} - \mathrm{si}(\nu a) + i\,\mathrm{Ci}(\nu a)$$

$$-i(C + \log 2\nu a) + ie^{2i\nu a}\,\{\mathrm{Ci}(2\nu a) - \mathrm{Ci}(\nu a)$$

$$-i\,\mathrm{si}(2\nu a) + i\,\mathrm{si}(\nu a)\}\Big]\,,$$

and, for I_2, the total is:

$$I_2 = \frac{1}{\nu}\Big[\frac{\pi}{2} - \mathrm{si}(\nu a) + i\,\mathrm{Ci}(\nu a) - i(C + \log 2\nu a)$$

$$+ i\,e^{2i\nu a}\,[\mathrm{Ci}(2\nu a) - \mathrm{Ci}(\nu a) - i\,\mathrm{si}(2\nu a) + i\,\mathrm{si}(\nu a)]\Big]\,.$$

We now combine these partial results to obtain for the integral of $f(x-i0)$:

$$\int_{-a}^{a} f(x-i0)\,dx = \frac{P}{\pi i\rho\omega\nu}\Big[2\pi i\nu a + 2i[C + \log 2\nu a + g(2\nu a)]$$

$$- 4\pi i e^{-i\nu a}\sin\nu a\Big]\,.$$

We have again used the fundamental relations between the Ci and si functions and the standard auxiliary functions $f(\nu a)$ and $g(\nu a)$ given in Abramowitz and Stegun (1964).

Finally, we obtain for $\bar{\eta}\cos(\omega t + \delta)$:

$$\bar{\eta}\cos(\omega t+\delta) = \frac{2P}{\rho g\nu a}\Big[\frac{1}{2\pi}[C + \log 2\nu a + g(2\nu a)]$$

$$- \sin\nu a\cos\nu a\Big]\sin\omega t$$

$$+ \frac{2P}{\rho g\nu a}\Big[\sin^2\nu a\Big]\cos\omega t\,.$$

This equation implies then that:

$$\bar{\eta}\cos\delta = \frac{2P}{\rho g\nu a}\sin^2\nu a\,;$$

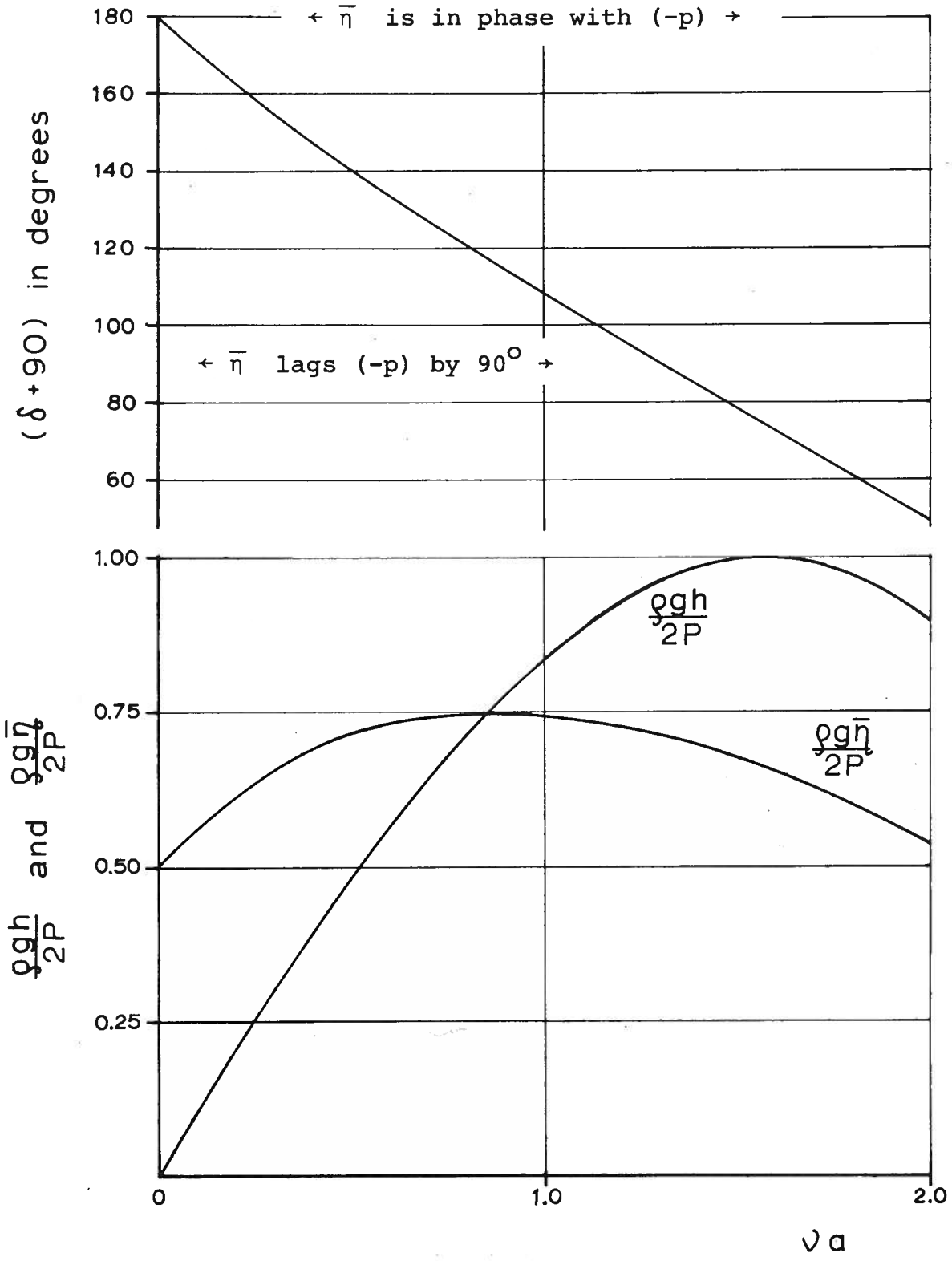

Figure 15. Average surface elevation under box: Phase and amplitude. Also, amplitude of generated waves at infinity.

$$\bar{\eta} \sin \delta = \frac{2P}{\rho g \nu a} \{\sin \nu a \cos \nu a - \frac{1}{2\pi}[C + \log 2\nu a + g(2\nu a)]\} \quad .$$

Figure 15 shows the results predicted by these formulas. The mean amplitude of the surface displacement in the wavemaker, $\bar{\eta}$, is actually less than the amplitude of the generated waves under a considerable range of conditions. The latter amplitude has been denoted by h in the figure; the curve is the same as the basic sine curve corresponding to the case $b/a = 0.0$ in Figure 7. It should not be implied, of course, that the surface elevation is uniform across the width of the wavemaker. The quantity $\bar{\eta}$ is the *mean* amplitude of motion in the wavemaker. The amplitude of surface displacement could be much greater locally than indicated by the value of $\bar{\eta}$.

Figure 15 also shows how the mean surface motion in the wavemaker lags behind the exciting force. At very low frequency, the surface moves downward as the pressure increases, so that there is a 180° phase difference between surface position and pressure. For higher frequencies, the surface motion lags more and more. At a value of νa just a short distance off the figure toward the right, the surface motion will be exactly in phase with the pressure, which means that the surface moves upwards as the pressure increases.

UNCLASSIFIED

Security Classification

DOCUMENT CONTROL DATA - R & D

(Security classification of title, body of abstract and indexing annotation must be entered when the overall report is classified)

1. ORIGINATING ACTIVITY (Corporate author)

UNIVERSITY OF MICHIGAN, Dept. of Naval Arch. and Marine Eng., Ann Arbor, Mich. 48104

2a. REPORT SECURITY CLASSIFICATION

UNCLASSIFIED

2b. GROUP

3. REPORT TITLE

OSCILLATING PRESSURE FIELDS ON A FREE SURFACE

4. DESCRIPTIVE NOTES (Type of report and inclusive dates)

Interim Technical Report 1 March 69 to 31 July 1969

5. AUTHOR(S) (First name, middle initial, last name)

T. Francis Ogilvie

6. REPORT DATE

September 1969

7a. TOTAL NO. OF PAGES

57

7b. NO. OF REFS

5

8a. CONTRACT OR GRANT NO.

N00014-67-A-0181-0016

b. PROJECT NO.

SR 009 01 01

c.

d.

9a. ORIGINATOR'S REPORT NUMBER(S)

No. 030
(Dept. of Naval Architecture and Marine Engineering)

9b. OTHER REPORT NO(S) (Any other numbers that may be assigned this report)

None

10. DISTRIBUTION STATEMENT

This document has been approved for public release and sale; its distribution is unlimited.

11. SUPPLEMENTARY NOTES

12. SPONSORING MILITARY ACTIVITY

Naval Ship Research and Development Center, Washington, D. C. 20007

13. ABSTRACT

The effect of a vertical barrier or lip on the wave generating capability of a pneumatic wavemaker is analyzed. For lip immersion approaching zero, the wave amplitudes approach the values predicted by Stoker in 1957. For finite lip immersion, wave amplitude is generally reduced below the amplitude from a wavemaker with no lip, but under certain conditions the amplitude can be greatly increased by the lip. Numerical results are presented. These results are used to show that the effect of sidewalls will be generally negligible in predicting the added mass and damping per unit length of a long air-cushion vehicle with sidewalls (captured-air-bubble vehicle). Such effects then being neglected, the added mass and damping are computed as functions of frequency and conditions of static support. The amplitude and phase of the mean free surface motion under the vehicle are also computed. It is found that the surface motion can actually be exactly opposite to that expected from quasi-static considerations.

DD FORM 1 NOV 1473

UNCLASSIFIED

Security Classification

14. KEY WORDS	LINK A		LINK B		LINK C	
	ROLE	WT	ROLE	WT	ROLE	WT
Wavemakers						
Captured-Air-Bubble Vehicles						
Ship Motions						
Water Waves						

University of Michigan, Department of Naval Architecture and Marine Engineering.

OSCILLATING PRESSURE FIELDS ON A FREE SURFACE, by T. Francis Ogilvie. July 1969. 57pp., 5 refs.

The effect of a vertical barrier or lip on the wave generating capability of a pneumatic wavemaker is analyzed. For lip immersion approaching zero, the wave amplitudes approach the values predicted by Stoker in 1957. For finite lip immersion, wave amplitude is generally reduced below the amplitude from a wavemaker with no lip, but under certain conditions the amplitude can be greatly increased by the lip. Numerical results are presented. These results are used to show that the effect of sidewalls will be generally negligible in predicting the added mass and damping per unit length of a long air-cushion vehicle with sidewalls (captured-air-bubble vehicle). Such effects then being neglected, the added mass and damping are computed as functions of frequency

Wavemakers
Captured-Air-Bubble Vehicles
Ship Motions
Water Waves

University of Michigan, Department of Naval Architecture and Marine Engineering.

OSCILLATING PRESSURE FIELDS ON A FREE SURFACE, by T. Francis Ogilvie. July 1969. 57pp., 5 refs.

The effect of a vertical barrier or lip on the wave generating capability of a pneumatic wavemaker is analyzed. For lip immersion approaching zero, the wave amplitudes approach the values predicted by Stoker in 1957. For finite lip immersion, wave amplitude is generally reduced below the amplitude from a wavemaker with no lip, but under certain conditions the amplitude can be greatly increased by the lip. Numerical results are presented. These results are used to show that the effect of sidewalls will be generally negligible in predicting the added mass and damping per unit length of a long air-cushion vehicle with sidewalls (captured-air-bubble vehicle). Such effects then being neglected, the added mass and damping are computed as functions of frequency

Wavemakers
Captured-Air-Bubble Vehicles
Ship Motions
Water Waves

University of Michigan, Department of Naval Architecture and Marine Engineering.

OSCILLATING PRESSURE FIELDS ON A FREE SURFACE, by T. Francis Ogilvie. July 1969. 57pp., 5 refs.

The effect of a vertical barrier or lip on the wave generating capability of a pneumatic wavemaker is analyzed. For lip immersion approaching zero, the wave amplitudes approach the values predicted by Stoker in 1957. For finite lip immersion, wave amplitude is generally reduced below the amplitude from a wavemaker with no lip, but under certain conditions the amplitude can be greatly increased by the lip. Numerical results are presented. These results are used to show that the effect of sidewalls will be generally negligible in predicting the added mass and damping per unit length of a long air-cushion vehicle with sidewalls (captured-air-bubble vehicle). Such effects then being neglected, the added mass and damping are computed as functions of frequency

Wavemakers
Captured-Air-Bubble Vehicles
Ship Motions
Water Waves

University of Michigan, Department of Naval Architecture and Marine Engineering.

OSCILLATING PRESSURE FIELDS ON A FREE SURFACE, by T. Francis Ogilvie. July 1969. 57pp., 5 refs.

The effect of a vertical barrier or lip on the wave generating capability of a pneumatic wavemaker is analyzed. For lip immersion approaching zero, the wave amplitudes approach the values predicted by Stoker in 1957. For finite lip immersion, wave amplitude is generally reduced below the amplitude from a wavemaker with no lip, but under certain conditions the amplitude can be greatly increased by the lip. Numerical results are presented. These results are used to show that the effect of sidewalls will be generally negligible in predicting the added mass and damping per unit length of a long air-cushion vehicle with sidewalls (captured-air-bubble vehicle). Such effects then being neglected, the added mass and damping are computed as functions of frequency

Wavemakers
Captured-Air-Bubble Vehicles
Ship Motions
Water Waves

and conditions of static support. The amplitude and phase of the mean free surface motion under the vehicle are also computed. It is found that the surface motion can actually be exactly opposite to that expected from quasi-static considerations.

and conditions of static support. The amplitude and phase of the mean free surface motion under the vehicle are also computed. It is found that the surface motion can actually be exactly opposite to that expected from quasi-static considerations.

and conditions of static support. The amplitude and phase of the mean free surface motion under the vehicle are also computed. It is found that the surface motion can actually be exactly opposite to that expected from quasi-static considerations.

and conditions of static support. The amplitude and phase of the mean free surface motion under the vehicle are also computed. It is found that the surface motion can actually be exactly opposite to that expected from quasi-static considerations.

University of Michigan, Department of Naval Architecture and Marine Engineering.

OSCILLATING PRESSURE FIELDS ON A FREE SURFACE, by T. Francis Ogilvie. July 1969. 57pp., 5 refs.

The effect of a vertical barrier or lip on the wave generating capability of a pneumatic wavemaker is analyzed. For lip immersion approaching zero, the wave amplitudes approach the values predicted by Stoker in 1957. For finite lip immersion, wave amplitude is generally reduced below the amplitude from a wavemaker with no lip, but under certain conditions the amplitude can be greatly increased by the lip. Numerical results are presented. These results are used to show that the effect of sidewalls will be generally negligible in predicting the added mass and damping per unit length of a long air-cushion vehicle with sidewalls (captured-air-bubble vehicle). Such effects then being neglected, the added mass and damping are computed as functions of frequency

Wavemakers
Captured-Air-Bubble Vehicles
Ship Motions
Water Waves

University of Michigan, Department of Naval Architecture and Marine Engineering.

OSCILLATING PRESSURE FIELDS ON A FREE SURFACE, by T. Francis Ogilvie. July 1969. 57pp., 5 refs.

The effect of a vertical barrier or lip on the wave generating capability of a pneumatic wavemaker is analyzed. For lip immersion approaching zero, the wave amplitudes approach the values predicted by Stoker in 1957. For finite lip immersion, wave amplitude is generally reduced below the amplitude from a wavemaker with no lip, but under certain conditions the amplitude can be greatly increased by the lip. Numerical results are presented. These results are used to show that the effect of sidewalls will be generally negligible in predicting the added mass and damping per unit length of a long air-cushion vehicle with sidewalls (captured-air-bubble vehicle). Such effects then being neglected, the added mass and damping are computed as functions of frequency

Wavemakers
Captured-Air-Bubble Vehicles
Ship Motions
Water Waves

+

University of Michigan, Department of Naval Architecture and Marine Engineering.

OSCILLATING PRESSURE FIELDS ON A FREE SURFACE, by T. Francis Ogilvie. July 1969. 57pp., 5 refs.

The effect of a vertical barrier or lip on the wave generating capability of a pneumatic wavemaker is analyzed. For lip immersion approaching zero, the wave amplitudes approach the values predicted by Stoker in 1957. For finite lip immersion, wave amplitude is generally reduced below the amplitude from a wavemaker with no lip, but under certain conditions the amplitude can be greatly increased by the lip. Numerical results are presented. These results are used to show that the effect of sidewalls will be generally negligible in predicting the added mass and damping per unit length of a long air-cushion vehicle with sidewalls (captured-air-bubble vehicle). Such effects then being neglected, the added mass and damping are computed as functions of frequency

Wavemakers
Captured-Air-Bubble Vehicles
Ship Motions
Water Waves

University of Michigan, Department of Naval Architecture and Marine Engineering.

OSCILLATING PRESSURE FIELDS ON A FREE SURFACE, by T. Francis Ogilvie. July 1969. 57pp., 5 refs.

The effect of a vertical barrier or lip on the wave generating capability of a pneumatic wavemaker is analyzed. For lip immersion approaching zero, the wave amplitudes approach the values predicted by Stoker in 1957. For finite lip immersion, wave amplitude is generally reduced below the amplitude from a wavemaker with no lip, but under certain conditions the amplitude can be greatly increased by the lip. Numerical results are presented. These results are used to show that the effect of sidewalls will be generally negligible in predicting the added mass and damping per unit length of a long air-cushion vehicle with sidewalls (captured-air-bubble vehicle). Such effects then being neglected, the added mass and damping are computed as functions of frequency

Wavemakers
Captured-Air-Bubble Vehicles
Ship Motions
Water Waves

and conditions of static support. The amplitude and phase of the mean free surface motion under the vehicle are also computed. It is found that the surface motion can actually be exactly opposite to that expected from quasi-static considerations.

and conditions of static support. The amplitude and phase of the mean free surface motion under the vehicle are also computed. It is found that the surface motion can actually be exactly opposite to that expected from quasi-static considerations.

and conditions of static support. The amplitude and phase of the mean free surface motion under the vehicle are also computed. It is found that the surface motion can actually be exactly opposite to that expected from quasi-static considerations.

and conditions of static support. The amplitude and phase of the mean free surface motion under the vehicle are also computed. It is found that the surface motion can actually be exactly opposite to that expected from quasi-static considerations.